FINITE ELEMENT MODELLING OF HEAT DAMAGED CONCRETE EXTERNALLY BONDED WITH GFRP LAMINATE

A thesis submitted in the partial fulfillment of the requirements for the award of the degree of

MASTER OF ENGINEERING
IN
STRUCTURAL ENGINEERING

BY

ANSHUL SANDHU

801724005

UNDER THE SUPERVISION OF

DR. A. B.DANIE ROY
Assistant Professor

DR. REEMA GOYAL
Lecturer

CIVIL ENGINEERING DEPARTMENT
THAPAR INSTITUTE OF ENGINEERING & TECHNOLOGY
(A DEEMED TO BE UNIVERSITY)
PATIALA, PUNJAB

JULY, 2019

DECLARATION

I, Anshul Sandhu, hereby declare that the work presented in this thesis entitled **"Finite Element Modelling Of Heat Damaged Concrete Externally Bonded With GFRP Laminate"** in fulfillment of the requirement for the award of degree of **Master of Engineering** in **Structures**, submitted at **Civil Engineering Department**, **Thapar Institute of Engineering & Technology**, **Patiala**, is an authentic record of work carried out under the guidance of **Dr. A. B. Danie Roy, Assistant Professor and Dr. Reema Goyal, Lecturer**, **Thapar Institute of Engineering & Technology**, **Patiala.** The matter presented in this has not been submitted either in part or full to any other university or institute for the award of any other degree.

Date: 5/9/2019

(Anshul Sandhu)

(801724005)

CERTIFICATE

This is to certify that the above declaration made by the student concerned is correct according to the best of my knowledge and belief.

Date: 5/9/19

Dr. A. B.Danie Roy
Assistant Professor,
Department of Civil Engineering,
Thapar Institute of Engineering and
Technology, (A deemed to be University)
Patiala, Punjab.

Date: 5/9/19

Dr. Reema Goyal
Lecturer,
Department of Civil Engineering,
Thapar Institute of Engineering and
Technology, (A deemed to be University)
Patiala, Punjab.

ACKNOWLEDGMENT

In the accomplishment of this dissertation successfully, many people have bestowed upon me their blessings and the heart pledged support, this time I am utilizing to thank all the people who have been concerned with this dissertation. It would not be fair on my part if I don't say a word of thanks to all those whose sincere advice made this period an educative, enlightening, pleasurable and memorable one.

Primarily, I would like to express my special thanks of gratitude to **Dr. A. B. Danie Roy**, **Assistant Professor**, Department of Civil Engineering, Thapar Institute of Engineering and Technology, Patiala, for providing his valuable guidance and support that helped me patch this project report and make it a full proof success. His suggestions and instructions have served as the major contributor to the completion of the dissertation.

I would like to extend my deep gratitude to **Dr. Reema Goyal, Lecturer**, Department of Civil Engineering, Thapar Institute of Engineering and Technology, Patiala, for her gracious efforts and keen pursuits which have remained as a valuable asset for the successful completion of the dissertation. Her timely advice, meticulous scrutiny and scholarly advice have helped me to a great extent to accomplish this task.

I would like to extend my sincere gratitude to **Dr. Prem Pal Bansal, Associate Professor** and Head of Department of Civil Engineering, Thapar Institute of Engineering and Technology, Patiala for his kind cooperation and encouragement which has always been a boost.

Last but not least, I would like to thank my family and friends for their constant encouragement during the entire period of work.

Anshul Sandhu
(801724005)

ABSTRACT

Given the extreme occurrences of natural disasters (earthquakes or storms) and accidents (fire or explosion), over the past century repairing and enhancing of current concrete constructions has become more prevalent owing to increasing understanding and confidence in the use of sophisticated composite repair products. The previous experience of actual fires demonstrates that it is unusual for concrete construction to collapse due to fire and that most fire-damaged concrete buildings can be economically repaired rather than being totally replaced or demolished. Due to their high strength-to-weight and stiffness-to-weight ratios, corrosion resistance, lightweight and moderately high durability, simple installation and low labor costs, the use of fiber-reinforced polymer (FRP) composites has achieved popularity among the reinforcing products. Two popular methods in the FRP implementation for reinforcement are. The former is widely used for purposes of strengthening, while the latter is also becoming popular day by day. Partial or full damage of concrete members due to accidental fire – that is at elevated temperature – often leads to a significant reduction in the strength of concrete. The strength of such heat-damaged concrete structural members may be improved partly by the application of FRP composites – either by wrapping as whole or bonding locally on external surfaces. Both require an understanding of the bond characteristics of FRP laminates with heat-damaged concretes. Also, recent research has attempted to simulate the behavior of reinforced concrete structures strengthened with FRP composites using the finite element method (FEM). In the present study, finite element modeling of a heat damaged concrete specimen externally bonded with the GFRP Laminate is carried out with the help of commercially available software ANSYS 15.0. The results of the Finite Element Model are compared with the experimental results which were done by the researcher. It is found that the values of Load vs Slip obtained in ANSYS are close to the Load vs Slip values obtained from the experimental study.

TABLE OF CONTENTS

LIST OF TABLES

LIST OF FIGURES

LIST OF ABBREVIATIONS

AFRP	Aramid Fibre Reinforced Polymers
CFRP	Carbon Fibre Reinforced Polymers
EBR	Externally bonded retrofit
FEA	Finite Element Analysis
FEM	Finite Element Method
FRP	Fiber-reinforced plastic
GFRP	Glass Fibre Reinforced Polymers
IS	Indian Standard
NSMR	Near surface mounted FRP retrofit
Tg	Transition Temperature

CHAPTER 1

INTRODUCTION

1.1 GENERAL

Recently, the rehabilitation and upgrade of current civil engineering facilities have become a significant problem which often needs instant attention from asset managers. The primary reasons for structural reinforcement include upgrading capacity to withstand miscalculated loads, growing load carrying capacity for higher permit loads, eliminating premature failure due to inadequate detailing, restoring load carrying capacity due to heat or fire, corrosion and other degradation related to aging, etc. In concrete constructions, heating or fire incidents often require repair and recovery. Concrete structures such as chemical industrial structures, cement plant clinker silos, nuclear reactor vessels, warm crude oil storage tanks, glass-making industrial structures, reinforced concrete chimneys and high-rise buildings in case of accidental fire are often subjected to high temperatures. The collapse of concrete structures during a fire is very rare, and reparation of concrete structures after the fire is typically an economical and feasible alternative compared to demolition and reconstruction.

Many reinforced concrete, masonry and steel structures are built yearly around the world. Because of their aging and the environmental impacts, many of them deteriorate or may become unsafe to use due to modification in usage, changes in loading, inferior building material used or natural disasters. It is preferable to repair/retrofit an RC structure than to demolish taking economic and environmental factors into account. There are few situations where, due to the absence of rigidity, durability, ductility, and strength, a prevalent structure would require better reinforcement or restoration.

Some fundamental conditions by which a structure needs to be strengthened in the midst of its life expectancy are:

- Seismic retrofitting as required by the code
- Deficiencies in the initial design period
- Modification in usage

These flaws can be repaired and reinforced by several widely used methods and materials, depending on the required properties, use, and extent of damage in structural elements. Owing to their high stiffness-to-weight ratio, strength-to-weight ratio, better corrosion resistance, high durability and lightweight, the use of fiber-reinforced polymer (FRP) composites has expanded its popularity among the reinforcing materials. Fiber-reinforced plastic (FRP) is a compound material made of a fiber-reinforced polymer matrix with an adequate aspect ratio (length to thickness) of fibres to provide significant strengthening in one or more directions. The fibres function as the primary components of reinforcement whereas the polymer matrix (epoxy resins) acts as a binder which guards the fibres and transfers forces to and between the fibres.

FRP composites differ from traditional building materials like steel or aluminum. The former are anisotropic meaning apparent properties in the direction of the load applied, while the latter are isotropic meaning uniform properties in all directions, regardless of the load applied. The composite characteristics of FRP are therefore directional, suggesting that the highest mechanical characteristics are towards fiber positioning.

1.2 MATERIALS FOR FRP STRENGTHENING

The three primary parts of an FRP reinforcement scheme, namely fibres, matrices, and adhesives are briefly discussed here:

1.2.1 Fibres

Three kinds of fiber reinforcement are generally used to reinforce civil engineering structures, namely Carbon, Glass and Aramid fibres. Unidirectional FRP materials, when loaded in direct tension, display a linear-elastic stress-strain relationship without yielding or plastic behavior until failure. Since the fibre in an FRP material is the primary load-bearing element, fiber kind, fibre alignment, and fabric thickness (fiber amount) influence the tensile strength and rigidity. Figure 1.1 compares stress-strain behavior for various unidirectional FRPs with steel. Carbon is the stiffest, while at failure Glass and Aramid have a longer elongation. All fibres show a linear elastic behavior up to failure, while a definite yield limit exists for mild steel.

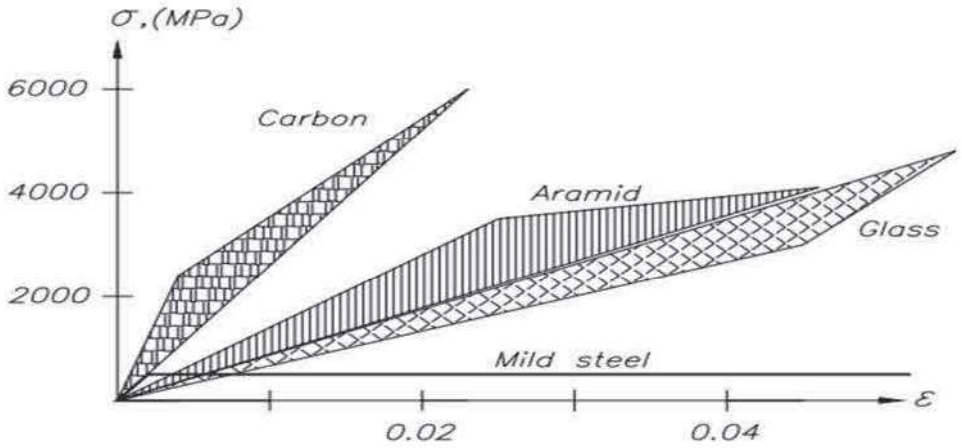

Figure 1.1 Comparison of Stress-strain behavior of various FRPs with mild steel (Täljsten, B., 2002)

Glass fibre is an inorganic fiber produced by melting methods which consist melting of suitable combination of raw materials, sand calcareous and alumina. Typical fibre diameters range between 8 - 25 μm.Glass fibers are categorized into three kinds (FIB Bulletin 14, 2001) which are as follows:-

- E- Glass fibres
- S- Glass fibres
- AR- Glass fibres (Alkali resistant).

E-glass is ideal for structural applications of general use. It also has great heat and electrical resistance. The low alkali strength of E - Glass fibres is unfavorable. S- Glass or strength grade is a unique glass with greater tensile strength and modulus along with decent heat resistance. S-glass has better protection to acids such as H_2SO_4, HCL, and HNO_3 compared to E-glass, but it is still not alkali resistant. A significant quantity of zircon is added to create alkali-resistant glass, AR - glass, to avoid cement-alkali from eroding glass fibre. AR-glass has E – glass like mechanical characteristics.

Carbon fiber is defined as fibres with an 80-95 percent carbon content. Precursor products currently available to produce carbon fibres are polyacrylonitrile (PAN) fibres, rayon fibres, or pitch. The carbon fibers based on pitch offer overall purpose and materials of high strength/elasticity. The carbon fibers of the PAN type yield products of elevated strength and elevated elasticity. In particular, at room temperatures, humidity, atmosphere, solvents, bases or weak acids do not influence carbon fibres.

Aramid fibres were first introduced in 1971. Aramid is fatigue-resistant, static as well as dynamic. The diameter of the aramid fiber is approximately 12 μm. Because of its high toughness, aramid is used for impact resistance and ballistic resistance armor. In civil engineering structures, Aramid fiber applications include ropes, wires, curtain walls, floors and ceilings, pipes and pre-stressing tendons. Aramid fibers, however, are susceptible to elevated heat, moisture, and UV radiation and are often insulated before civil engineering use.

Since the fibers are unable to transmit loads from each other, they have restricted use in engineering applications themselves. However, when incorporated in a matrix material to form a compound, the matrix connects the fibers together, allowing loads to be transferred to the fibers and protecting them from environmental harm and handling damage (Agarwal and Broutman, 1990).

The matrix for structural composite materials may be either of the sort of thermosetting or of the sort of thermoplastic, the most common being the first. The matrix has a powerful impact on multiple composite mechanical characteristics such as transverse strength and modulus, compression and shear features. High strength matrices tend to be brittle. Polyester, Vinyl ester, and epoxy are the most frequently used polymer matrix materials used with high-performance fiber reinforcement. Polymers with excellent process capability and chemical resistance are thermosetting polymers. Though Epoxies are more costly than polyesters and Vinyl ester, they generally have excellent durability and better mechanical characteristics (FIB, Bulletin 14, 2001).

1.2.2 Composites

Fibres, matrix, and additives together form a Composite. FRP composites can be categorized based on the type of fibre used as follows:-

- Glass Fibre Reinforced Polymers(GFRP)
- Carbon Fibre Reinforced Polymers(CFRP)
- Aramid Fibre Reinforced Polymers(AFRP)

The usual fiber volume fraction in FRPs is about 50-70% for pultruded laminates and 25-35% for hand lay-up sheets. Practical applications and research work have made use of all the above laminates, but as far as the strengthening work is related first two has been used more commonly. CFRP composites have superior characteristics but are also considerably more expensive than GFRP composites. (Teng.et al.,2003).

1.2.3 Adhesive

An adhesive is any non-metallic material that is applied to one surface, or both surfaces, of two distinct products that bind and resist separation. The most prevalent structural adhesive in use is epoxy adhesives. Epoxy adhesive results from the mixing of hardener with an epoxy resin. The characteristics of epoxy adhesives depend primarily on the hardener used. Successful use of an epoxy scheme relies on the preparing of an appropriate specification that must include requirements such as adherent components, blending, application temperatures and methods, surface preparation, curing temperatures, creep characteristics, heat expansion, chemical resistance, and abrasion.

It is therefore of prime importance that the reinforcement systems should not be divided into separate parts such as the FRP material is coming from one supplier and the adhesive from a different supplier unless the systems have been thoroughly examined and evaluated together. Two distinct time notions required to be taken into account while using epoxy adhesives; pot life and the open time. Pot life is the moment after blending the resin and the hardener you can work with the adhesive before it begins to harden in the mixing container. Pot life can differ from a few seconds to some years for an epoxy adhesive. The time which we have at our disposal after applying the adhesive to the adherents and before joining them is called Open Time. Pot life and Open time for a typical epoxy adhesive at 20 °C are 20 - 90 minutes and 30 - 120 minutes, respectively.

The Transition Temperature, *Tg* is another significant parameter linked to epoxy. As most of the adhesives are polymer-based due to which they display polymer-like behavior. Transition in the polymers takes place at a certain temperature from comparatively hard to elastic glass-like materials to comparatively rubber-like material. This particular temperature level is described as the glass transition temperature and is distinct for various polymers.

1.3 FIBRE APPLICATION

Various areas where the FRP systems as a strengthening and retrofitting tool can be used as follow:

- Enhancement of the Flexural capacity
- Shear Enhancement, and
- Enhancement of column confinement and ductility.

In addition to above FRP systems have also been efficiently employed to seismically enhance the concrete structures. These applications include weakening the mechanism of brittle failure for e.g. shear failure of beams and columns or the beam column intersection. FRP systems also help in the confinement of the columns by resisting the buckling of the longitudinal bars. FRP composites can be used in almost all kinds of settings on internal and external structural elements due to the improved corrosion resistance ability.

(a) (b)

(c)

Figure 1.2 FRP Application on (a) Beams , (b) Slabs and (c) Columns.
(https://www.structuremag.org/?p=8643)

Externally bonded FRP retrofit and Near surface mounted FRP retrofit are two regular methods in the application of FRP for reinforcement purposes. The former is commonly used for enhancing reasons, while the latter is also becoming increasingly popular every day. EBR method consists of retrofitting with the use of either FRP sheets or Laminates while in NSMR system there are slots/grooves in the concrete cover region of the structure which houses the rectangular or circular rods and even plates of limited width. The bond between the rods or plates

and the slots is achieved with the help an epoxy adhesive or a cement grout of high quality. Simple Concept of both the method using FRP plate is shown in Figure 1.3.

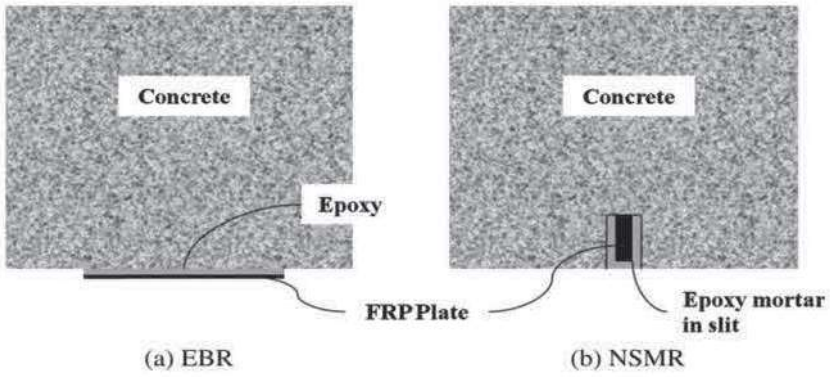

Figure 1.3 Concept of EBR and NSMR (S.-Y. Seo et al., 2013)

No one structural enhancement technique suits all circumstances. The exterior of the structure is processed in an externally bonded retrofit method and either a pressure laminated plate is bonded to the surface or a field wet-layup FRP (Figure 1.4) composite is set up onto the structure in-situ.

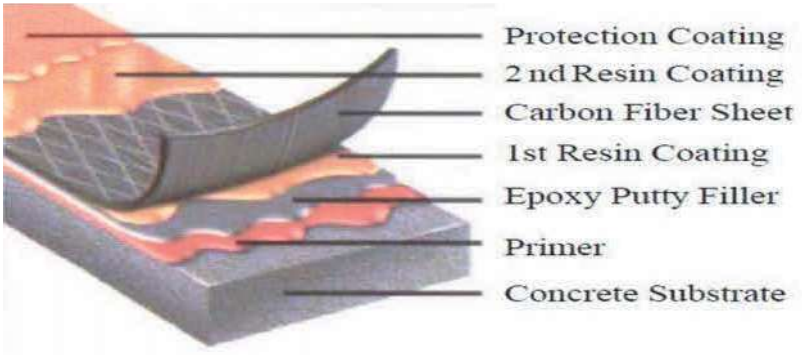

Figure 1.4 Wet layup system (Saito and Kobayashi, 2000)

Pros and Cons of both the FRP Strengthening method are discussed below:-

1.3.1 Externally bonded retrofit method

Pros:-

- Easy to prepare surfaces compared to cutting grooves in NSM
- Ease in performing the overhead surface preparation &setting up
- For irregular geometry, Wet lay-up can be used
- Verified bond pull-off tests can be performed directly away

Cons:-

- Specific learning is needed for wet-lay-up FRP
- Surface preparation highly influence the bond of FRP with concrete
- More vulnerable to fire and mechanical breakdown than NSM
- Debonding being a major failure limits its implementation

1.3.2 Near Surface Mounted Retrofit method

Pros:-

- Much efficient than externally bonded
- FRP material is Shielded in the Epoxy
- Better fire resistance due to epoxy shielding

Cons:-

- Overhead cutting of groves may be more difficult
- Testing of field quality assurance is not easy as in case of externally bonded FRP
- To facilitate the Slot/groove ample cover is essential.

The bond between the FRP structure and the concrete is vital irrespective of the implementation technique, therefore surface preparation is crucial. Before the installation of FRP system care should be taken to resolve existing deterioration or corrosion of internal reinforcement if present. If the care is not taken the prior installation of the FRP system it will lead to its failure due to delamination from the concrete surface inhibiting its usage ability to the full extent.

1.4 DEBONDING BEHAVIOUR AND FAILURE MODES OF THE FRP

Since the forces are transmitted from the concrete structure to the FRP composites through the interface bond, therefore the study of bond behavior of FRP is of extreme importance. The main obstacle in full use of the FRP Strengthening is premature debonding. Studies have shown that even though retrofitting with FRP improves overall load capacity and strength of the structure but due to untimely debonding, FRP strength is rarely fully utilized. Debonding is a sudden form of failure where, owing to the enhanced stress in the FRP-Concrete bond interface, the FRP material peels off the concrete surface.

Usually, this failure is very fragile and difficult to forecast. Figure 1.5 shows the path of debonding progression which takes the least resistant path and depends on the characteristics of FRP, Interface and concrete substrate.

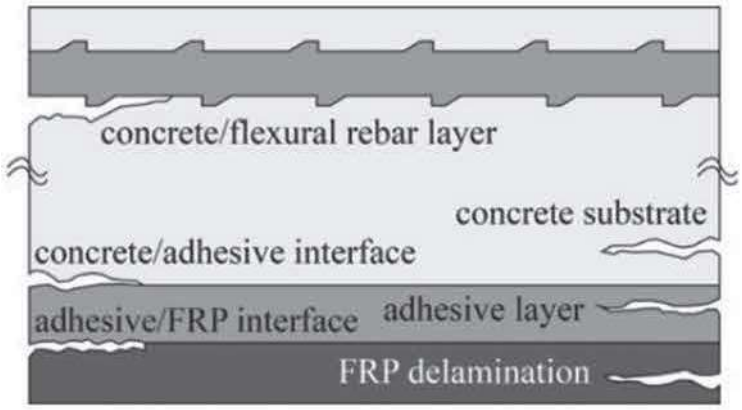

Figure 1.5 Path of Debonding Propagation (Kang et al. 2012)

In order to create models that could assist engineer plan against such abrupt failure, understanding of the FRP Concrete bond behavior is of utmost importance. To accomplish this, an experimental test is performed, generally, shear or beam experiments, and the information acquired is used to create a curve of bond-slip. The curve comprises an upward branch followed by a downward branch. One of the main points of creating a bond-slip curve is to assist in precisely determining the interfacial fracture energy, which impacts the ultimate strength of the FRP-concrete bond. The area below the bond-slip curve gives us the interfacial fracture energy.

In several types of research, premature debonding was categorized into two classifications:-

- Mid Span Debonding.
- End Plate Debonding

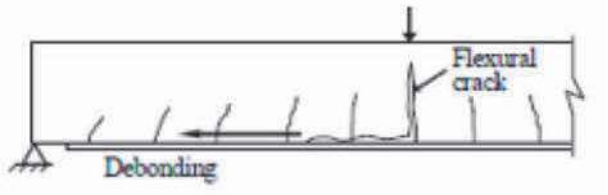

Figure 1.6 Mid Span Debonding (Teng et al. 2007)

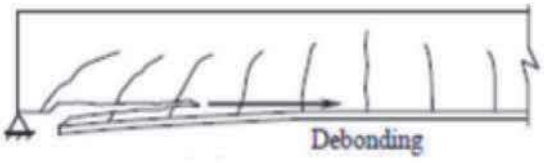

Figure 1.7 End Plate Debonding (Teng et al. 2007)

Mid-Span Debonding (Figure 1.6) happens at the center of the anchorage length owing to intermediate cracks triggered by an elevated bending moment in the center of the enhanced member while the End Plate Debonding (Figure 1.7) happens at the end of the FRP anchorage length. Main notable characteristics associated with early debonding involves concrete crushing in compression before the reinforcement yields, steel yielding in tension followed by FRP laminate rupture, concrete cover peels off and FRP getting debonded from concrete substrate. While the first two failure types are prevalent, the third sort usually occurs when thin FRP (< 1.0 mm) is attached to an irregular concrete substrate.

For the members strengthened by External Bonding, it was observed that debonding occurs at the immediate end of the FRP owing to the stress transfer from concrete to FRP. This not only leads to FRP debonding but also creates concrete diagonal cracks that assist in speeding up the debonding process. It is also seen that debonding of FRP relies on the physical and mechanical characteristics of FRP, concrete and adhesive epoxy (Mazzotti et al. 2007).

1.4.1 Failure Mode Classification

Because of the Brittle nature of the Concrete, FRP debonds from it in multiple respects that lead to sudden collapse owing to stress levels at the different locations along the length of the bond. In the occasion of Flexural and Shear enhancing dominant failure mode is debonding of FRP from the concrete substrate leading to the general failure of the structure. While in case of Column Wrapping fracture of the FRP Sheets is the dominant failure mode. Failure modes are shown in Figure 1.8 of an FRP Plate-bonded RC beam.

Some of the prominent failure modes are as follows:-

- Plate End Debonding: -This sort of debonding (Figure 1.8.e) is triggered by high normal stress and shear stress which arises at the plate/sheet end, extending through concrete cover up to the internal reinforcement level. Normally, this sort of collapse is seen in

concrete beams with very thin FRP materials than the beam portion. Using transverse strengthening like U-FRP stirrups, this type of debonding can be regulated.

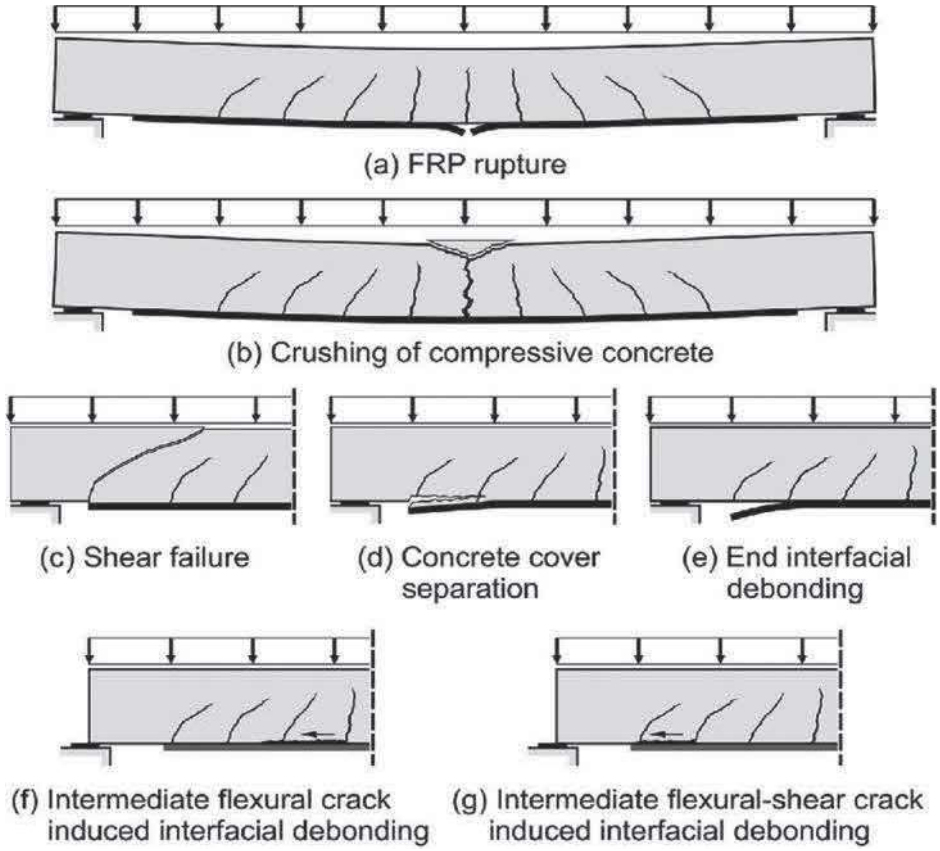

Figure 1.8 Failure modes of an FRP Plate-bonded RC beam. (Hind, M. Kh et al., 2016)

- Intermediate Crack-Induced Debonding: - This sort of debonding (Figure 1.8.f) is generally noticeable in the member's shear span and spreads towards the beam end, resulting in a concentration of large local strains. The release of tensile stress creates elevated interfacial stress between FRP and concrete after cracking. It is the most frequently observed failure mode; it is also recognized as Mode 1 (Pham et al. 2006 and Teng et al. 2007). This form of debonding can be reduced by continuous transverse strengthening.
- Axial Intermediate Crack Debonding:-This sort of debonding relates to straight pull test (most commonly single shear) where the FRP is exposed to tension contrary to the case of Bending Test where due to the beam curvature FRP is subjected to both Tension and Shear
- Critical Diagonal Crack Debonding: Comparable to crack-induced debonding even if it is associated with a single critical shear crack (Fig 1.8.c). The members with partial shear

reinforcement strengthened in flexure lead to this type of debonding. Failure is caused by the diagonal cracks intersecting the FRP.

- Concrete cover separation: - In this form of failure cracks are propagated along the concrete's tensile face. Cracks normally commence from the end of the plate and with the increase in load it widens more and more leading to separation (Figure 1.8.d) demonstrates a failure of this sort.

Although debonding failure remains a significant issue for FRP-bonded concrete structures, multiple latest types of research have given some alternatives for minimizing this form of flaw. For example, FRP sheets can be wrapped over the longitudinal FRP sheet around the concrete web, like U Transverse FRP Strips. Maintaining FRP width-to-thickness ratio greater than 50 can also help in reducing such failure as pointed out by Swamy et al (1995).

1.5 TYPES OF TEST TO STUDY THE FRP BOND BEHAVIOUR

As shown in Figure 1.9, the most frequently used experiment test setups for replicating FRP-concrete bond in the research can be widely classified into the following groups.

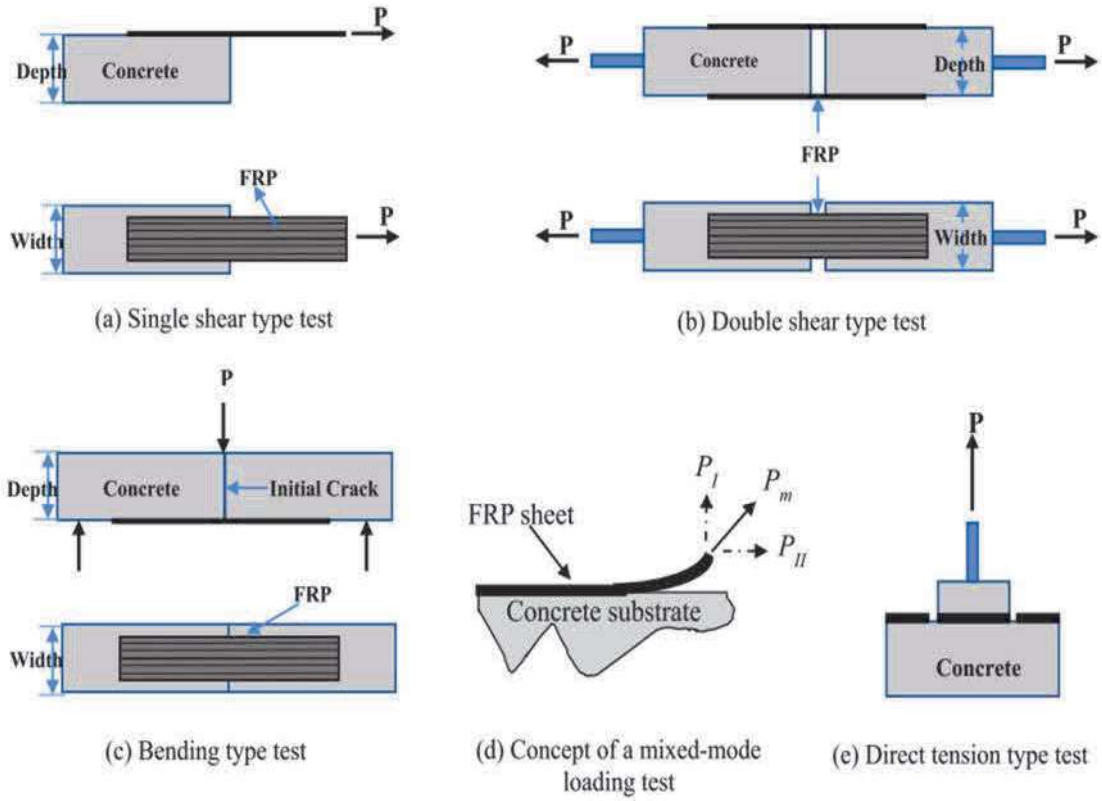

Figure 1.9 Various test to simulate the FRP-concrete bond (Mukhtar and Faysal, 2018)

- Single Shear Test: This is the most frequently used and easy to perform the experimental test setup used in the research field. In this Setup, FRP sheet attached on only one side of the prism or block with a suitable adhesive is subjected to the tensile force (Figure 1.9.a). Surface preparation of the Concrete prism is done using sandblasting, water jet or grinding machine before the application of adhesive in order to get rid of the weak mortar layer. The small length of the FRP sheet is left unattached at the edge to be able to avoid abrupt wedge breakdown.
- Double Shear Test: This test is identical to the single shear test with the solitary alteration that instead of one FRP Strip two FRP strip are bonded to the concrete specimen on the opposite faces of the concrete prism and is subjected to the tensile forces simultaneously (Figure 1.9.b). The surface of the concrete block is prepared in the same way as done in Single shear test along with the method of FRP bonding. To enable the implementation of the required force along each concrete block's length, a steel bar is inserted. A major problem in Double Shear Test arises due to the Eccentricity especially in cyclic loading where due to the sideways and rotational moment test results can be highly influenced.
- Bending Test: This test comprises of an FRP Strengthened Beam which is made to bend under the given loading (Figure 1.9.c).
- Mixed Mode Test: This test comprises both the shear and peeling impact on the FRP Concrete Bond Interface (Figure 1.9.d).
- Direct Tension Pull - off test: From the entire FRP Concrete Bond test this is the only test that can be performed on site. In this test steel plate is bonded on the FRP sheet attached to the concrete. A groove is cut on the around the steel plate and is subjected to a pull-out force (Figure 1.9.e).

1.6 CONCRETE SUBJECTED TO ELEVATED TEMPERATURE

Under ordinary circumstances, the majority of concrete constructions are subject to a temperature spectrum that is no more serious than that imposed by environmental conditions. There are significant instances, however, where these buildings can be subjected to much greater temperatures (e.g., Fire in the Building, Concrete building near the furnaces, Blasts from the aircraft engine jet blasts, building fires, and some accident circumstances related to nuclear power). During a fire, the temperature in buildings can reach up to 1100 ° C and sometimes even up to 1350 ° C in tunnels, resulting in serious harm to an overall concrete framework, thus jeopardizing the concrete element's bearing capacity. However, concrete is regarded a building

material that maintains its characteristics satisfactorily at elevated temperatures due to its small coefficient of thermal conductivity (slow motion of heat through concrete) as opposed to the steel that is susceptible to elevated temperatures. The temperature rise in the inner layers of the concrete is continuous under the effect of Elevated temperature. Since its a slow process, temperature gradients are generated due to the difference in temperature between the core and outer layers of the concrete causing extra harm to the element.

1.6.1 Mechanical characteristics of concrete under High Temperature:-

Concrete subjected to an elevated temperature (e.g. owing to accidental fire etc.) leads to significant decay and causes a number of transitions and reactions, resulting in progressive decomposition of the cement gel composition, lowering the durability, increase in drying shrinkage, structural cracking and related color change of the aggregate. High-temperature exposure to concrete impacts its mechanical and physical characteristics.

1.6.2 Effect on Compressive Strength:-

Resisting the collapse is one significant criterion for the building under fire. Resistance to collapse is greatly influenced by the Strength – Temperature characteristics of concrete. The decrease in strength is inevitable for all types of concretes but the pace of decrease varies with the kind of aggregate used.

For the concrete subjected to high temperature, three primary phases of compressive strength are as follows:-

- For Temperature variation from Room to 300 °C, Compressive strength remains constant or there can be a mild increase in it.
- For Temperature variation from 300°C to 800 °C there is an abrupt decrease in Compressive strength of Concrete.
- For Temperature 800 °C afterward roughly all concrete compressive strength is lost.

For the concrete with siliceous aggregates, this decrease in compressive strength is much more prominent. Rapid expansion in volume takes place at high temperatures leading to splitting/ spalling of the concrete. Lightweight aggregates have superior insulation characteristics owing to the heating process which they normally undergo during manufacturing. In light-weight concrete, the physical compatibility between aggregate and matrix in terms of deformability and expansion features is much better than in dense concrete, resulting in much less harm and internal stress during drying.

During heating, calcareous aggregates do not normally undergo physical modifications and are generally safe from splits and local damage. But some chemical changes take place at extremely elevated temperatures. The volume expansion creates splits and damage during the drying process.

1.6.3 Flexural Strength, Splitting Tensile strength and Modulus of Elasticity

Similar to compressive strength, there is also a decrease in concretes flexural strength, tensile strength and elastic modulus with temperature rise, but at an almost linear rate. The reduction in elasticity modulus induced by exposure to high temperatures is more pronounced than the reduction in compressive strength.

1.6.4 Stress-Strain Relationship

Stress-Strain curves have been found to become flattered with the rise in temperature and the maximum stress moving towards down and right. This shows that maximum stress and concrete elasticity modulus reduces as temperature rises, but the strain at peak stress rises as temperature rises.

1.7 FINITE ELEMENT METHOD (FEM)

Initially launched by Turner et al. (1956), the Finite Element Analysis (FEA) approach is a strong computing method for approximate solutions to a multitude of "real-world" engineering issues with complicated regions subject to particular border circumstances. Finite element analysis is basically a numerical method in which all the problem complications are maintained as they are such as loads, boundary conditions and varying shape but approximate solutions are obtained. Civil engineers use this technique widely to analyze space structures, beams, folded plates, shells, issues with rock mechanics, foundations and liquid flow assessment via porous media. Finite element assessment can handle both static and dynamic issues.

A complicated region describing a range is discretized into elementary geometric forms termed finite elements in the Finite Element Analysis Method. Over these elements, the material characteristics and the prevailing correlations are weighed and depicted at the element corner in terms of unknown values. A set of equations is formed during the assembly process s appropriately considering the conditions such as loading and constraints. These equations solution gives us the continuum's approximate behaviour.

1.7.1 General Explanation of the Method

There are certain fundamental unknowns in engineering problems. If they are established it is possible to predict the behavior of the entire structure. These fundamental unknowns are such as for solid mechanics it is displacements, for heat flow problems it is temperature and for fluid mechanics it is velocity.

Those unknowns are infinite in a continuum. The finite element method decreases these nonentities to a finite amount by separating the target range into tiny parts termed Elements and representing the unknown field variables within each element in terms of presumed approximating function (Interpolating / Shape function). Specified points called as nodal points or nodes are used to define the approximating functions in terms of field variables. Thus field variables of the nodal points are the unknowns in the finite element analysis. Once these field variables at the nodes are discovered, then with the help of interpolation functions field variables can be found at any point.

Next stage in finite element analysis, after the selection of elements and nodal unknowns, is the assembly of element properties for each element. For instance, we have to discover the force-displacement features of each individual component in solid mechanics, i.e. stiffness properties. This relation in mathematical term can be written as below:-

$$[k]_e\{\delta\}_e = \{F\}_e$$

Where $[k]_e$denotes the element stiffness matrix, $\{\delta\}_e$ denotes the element's nodal displacement vector and $\{F\}_e$ denotes the nodal force vector. The element k_{ij} of stiffness matrix symbolizes the force in coordinate direction '*i*' owing to a unit displacement in coordinate direction '*j*'. For formulating these element characteristics, there are four techniques accessible such as Direct method, weighted residual method, variational method and approach to energy equilibrium. Any of these techniques can be used to assemble characteristics of elements. Variation al approach is the more frequently employed method in solid mechanics for the assembly of nodal force vector and stiffness matrix.

To obtain the system equations$[k]\{\delta\} = \{F\}$, element characteristics are used to assemble structure / global. Boundary conditions are imposed thereafter. Nodal Unknowns are obtained after solving these simultaneous equations. Additional calculations are done using these nodal

unknowns to obtain the necessary values such as Moment, Stress, Strain etc in solid mechanics problems.

Therefore the different stages employed in the finite element analysis are summarized below:-

- Choose the appropriate elements and field variables
- Discretization of the domain.
- Choose the interpolation functions.
- Find the characteristics of the elements.
- Obtain global properties by assembling the element properties.
- Implementation of the boundary conditions.
- Obtain the nodal unknowns by solving the system equations.
- Make extra calculations to obtain the values needed.

As illustrated in Figure 1.10, through the discretization of domain/continua of concern into elements any practical engineering problem can be transformed into a mathematical representation. Such elements are linked by their "common" nodes to one another. A node indicates the place of the coordinate in a space. The degrees of freedom of the element are called nodal variables allocated to an element.

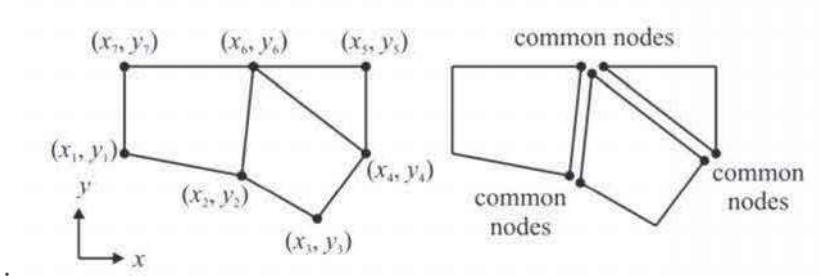

Figure 1.10 Discretization of continua into elements (Madenci and Guven, 2015)

Continuity for the nodal variables or degrees of freedom is provided with the common nodes. The element type and the physical aspect of the issue dictate the Degrees of freedom (DOF) of a node.

Depending on the physical aspect of the issue and the geometry, continua of concern can be discretized with the help various elements such as volume, area and line elements. Figure 1.11 shows a few of the prevalent elements used in Finite Element Analysis.

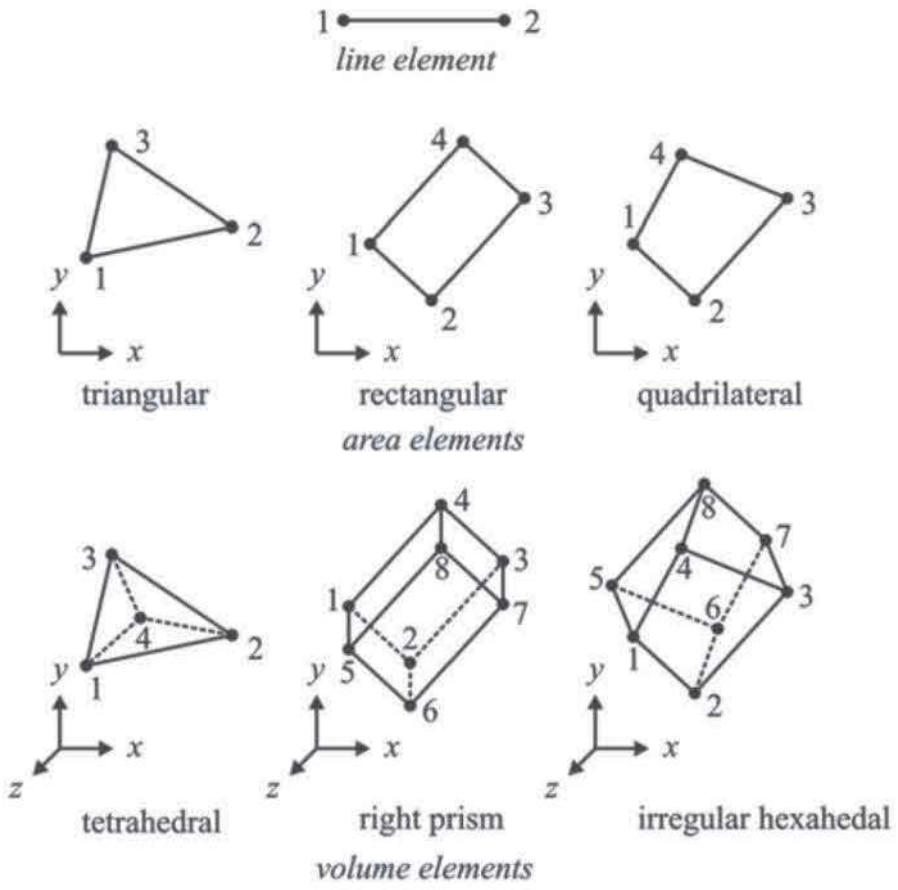

Fig 1.11 Various Elements along with node numbers (Madenci and Guven, 2015)

1.8 THESIS OBJECTIVE AND ITS ORGANIZATION

Finite elements Analysis offers a strong tool for investigating FRP Concrete Bond's complicated behavior with regard to being much quicker and highly cost-effective relative to the experimental studies.

- The aim of the thesis is to carry out the Finite Element Modelling for the bond at the Concrete FRP interface.
- To study the influence of elevated temperature on Load vs Slip behaviour along with its comparison to the experimental study to verify the accuracy of the modeling.
- To study the variation of ultimate bond strength with the bond length of GFRP.

The thesis was arranged in five chapters as below.

Chapter – 1: It addresses the general introduction related to the thesis topic.

Chapter – 2: The review of literature is presented in this chapter. It consists of a brief review of the Experimental procedures, Bond-Related Analytical Models and Finite Element Models related to FRP Concrete Bond Behaviour.

Chapter – 3: It deals with the procedure of modeling of Externally Bonded GFRP Laminate with Heat Damaged Concrete using a commercial finite element analysis package ANSYS 15.0. Types of Elements which were used to generate the model, properties used, meshing and boundary condition all have been discussed in this chapter.

Chapter – 4: It addresses the results/outcomes of the current study.

Chapter – 5: It provides the findings/conclusions from this study. The Future scope of work is too provided in this section.

CHAPTER 2

LITERATURE REVIEW

In this section, the literature review is presented as follows: (1) Experimental studies; (2) Analytical Models; and (3) Finite Element Models related to the behaviour of FRP Concrete Bond.

2.1 BOND BEHAVIOUR OF EXTERNALLY BONDED FRP WITH NORMAL CONCRETE

Chajes et al. (1996) performed a single shear experiment to investigate the bond strength and force transfer characteristics of a plate bonded externally. To determine the effects of concrete strength, adhesive and surface preparation bond length were not varied while to assess the bond force transfer it was varied. For the surface preparation method used were None, Stone wheel grinding and Wirewheel abrading. Test results indicated two failures, failure of the concrete below the interface and the adhesive concrete interface failure (dominant being the former one). Ultimate bond strength is greatly impacted by preparation of the surface with best being the mechanically abrading. The composite plate roughening and cleaning also increases bonding. The transfer of force was mostly uniform owing to the linear decrease in strain across the bond length. Owing to the failure of the concrete below the interface being a major failure, ultimate strength was related proportionally to the concrete compressive strength. It was also concluded that the length of bond development exists farther which the load cannot be elevated at failure.

Arduini et al. (1997) performed experimental testing of reinforced concrete beams enhanced with FRP. A total of six beam samples were built. Beams B1 and B2 were not FRP strengthened; Beam B3 and B4 were having one layer, while B5 and B6 were having two layers of FRP reinforcement. To assist in Anchorage for the specimen B6, Steel plate of 100 mm width and 1.5 mm thick was wrapped at the end of CFRP. Beam specimens were subjected to 4 point bending condition. Test results showed the occurrence of first crack at mid-span in the initial linear phase and development of numerous cracks together with the increase in a strain of CFRP in the nonlinear phase. B1 and B2 failed by crushing of the concrete after yielding of bottom steel. Shear cracks began at the edge of the plates and spread parallel to the longitudinal steel through the concrete cover. The fragile concrete cover separation was shown by B3 and B4. B5 displayed

extra stiffness in cracked zone owing to the additional CFRP layer but ultimately failed by the partition of the concrete cover. With the assistance of metal plate in B6, this issue was decreased.

Arduini et al. (1997) in relation to the above experiment, also examined the outcomes of four 300 x 400 x 2500 mm reinforced concrete beams. Beam 1 was kept unstrengthened, whereas unidirectional flexible wet-layup CFRP sheets were implemented to the beam soffits of rest of the beams. Beam 2 consisted of one layer, while Beam3 and Beam 4 had 2 layers each. In addition to this Beam 4 also had CFRP sheet wrapped in the transverse direction. Beam 1 failed similarly to the B1. Beam 2 failed due to the rupture of the sheet, while Beam 3 failed due to the concrete cover debonding at load 2.5 times the plain section. Maximum load capacity was shown by Beam 4 displaying the effectiveness of transversely wrapped CFRP sheet.

Arduini and Nanni (1997) performed a parametric study for FRP repaired reinforced concrete beams. The first group of parameter referred to the geometry and the property of the member. Geometric parameters used was (*h/b)* ratios of the rectangular section (0.5,1,4). Properties of the member consisted of 20 MPa and 30 MPa concrete compressive strengths, Steel reinforcement ratio (q) 37.5 % of the balanced, shear reinforcement ratio ρ_v (0.003). The second set of parameters were related to material (FRP) used for repair such as the thickness of FRP t_p, the ratio of bond length shear span *(p/a)*. FRP thickness and its associated stiffness were significant in reducing the beam deflection. The ratio Bond length to shear span *(p/a)* highly impacts the ultimate strength. Strength wise there was no advantage to repair the beam for *(p/a)*< 0.65. The failure mode was always the fracture of FRP for FRP 0.1 mm dense, regardless of the *(p/a)*. The rupture occurred only for the lengthiest bonding length that is *(p/a)* = 0.95 for a thickness of 0.5 mm. Rest of the resulted in concrete cover separation, suggesting that by increasing the amount of FRP it is not feasibly possible to improve the flexural strength of the beam.

Miller, B. and Nanni, A.(1999) performed an experimental study to investigate strain distribution among the Carbon Fiber Reinforced Polymer (CFRP) sheets and concrete. The experiment's primary goal was to tackle the variables influencing the CFRP sheets and concrete bond which were (1) Bonded length, (2) Concrete Compressive strength and (3) stiffness/no. of plies of CFRP and the same were the variables of the test. The experimental setup consisted of performing a Bending Type Test on 18 inverted T shape plain concrete specimens. The beam was simply supported with a center top center span of 42 inches (1067 mm) with a notch at the center in order to assist the beam to crack at the midspan. A CFRP strip with width (2 inches),

thickness (0.0065 in) was bonded to the tension face of the beam. In order to force the failure on one end transverse sheet was placed. Peeling of the sheet was the main cause for the specimen's failure. From the test result, it was concluded that the ultimate load remains unaffected by both the bond length and the concrete strength. Bond strength increased with increasing the stiffness but not proportionally.

Bizindavyi and Neale (1999) performed a single shear test to examine fibre and resin systems interfacial behavior. Concrete blocks having a dimension of 150 x 50 x 400 mm with a compressive strength 42.5 MPa, splitting tensile strength 3.5 MPa and 33.5 Mpa of Elastic Modulus were employed. CFRP and GFRP laminates having a width of 25 mm were bonded to concrete prisms keeping resin thickness uniform of the order of 1-1.2 mm. Sand Blasting was used as a mean of Surface preparation. Test variables were the no. of plies, bond length, and thickness. Two failures observed were a rupture of the FRP and shearing of concrete under the bond surface. It was observed that in order to obtain the full tensile capacity of the compound, the bond length of 160 mm for the 1-ply GFRP, 260 mm for the 2-ply GFRP, 80 mm for the 1-ply CFRP, 220 mm for the 2-ply CFRP were sufficient. During the initial loading, strain decreased exponentially, once the crack was initiated strain distribution showed bilinear decreasing trend and during the final loading stages trend was more or less linear.

Nakaba et al. (2001) performed research on Double shear test to examine the bond behavior amongst FRP laminates and concrete. Test factors were fiber type and concrete. The test specimens were made up of concrete block with dimensions 100 x 100 x 600 mm. One side of the specimen was additionally wrapped by the FRP in order to force the delamination only on the other side of the specimen. Three types of fibre were chosen for the experiment namely carbon standard and high stiffness) and Aramid fibres. All samples were subjected to tensile force until complete bond system breakdown occurred. It was noticed that with the increase in stiffness of FRP peak load also increased. The thickness of the putty did not affect bond behavior significantly. From the Load vs displacement connection, it was noticed that the load in the specimens (with low stiffness carbon fiber and the Aramid fibre) becomes steady, while the displacement continues to grow. There was no excessive elongation for a specimen with standard carbon fibre, high stiffness carbon fibre and standard carbon fibre with high unit weight, thus reaching higher maximum loads. It was also concluded that the type of FRP did not affect the bond stress which was influenced by the concrete compressive strength.

Harmon et al. (2003) performed the four-point bending experimental test on five reinforced concrete beams strengthened with different fibre systems and resin. The dimensions of the beam specimen were 152.3 x 228.6 x 2133.6 mm. Two distinct fibers were chosen. The first one was a dry sheet consisting of unidirectional fibres having a 0.165 mm thickness. It had a tensile strength of 3.8 GPa and modulus of 227.5 GPa. The second fibre used was a cured laminate having a 0.635 mm thickness and 124.1 GPa of modulus. Beam 1 was the unstrengthened or control beam, Beams 2 and Beam 3 were strengthened with a single layer of CFRP, whereas Beams 4 and Beam 5 consisted of 2 layers of CFRP with staggered cut off points. Thin and stiff resin layer was used in Beam 2 for bonding, while thicker flexible bond layer was used in Beam 3. Beam 4 consisted of a thick flexible layer on the inner side and thin stiff layer on the outer side, and Beam 5 consisted of two thick flexible layers of CFRP. The test result showed that Beam 1 failed in by steel yielding. There was no increase in strength in Beam 2 which break down owing to delamination of CFRP at crack A. There was an increase in strength of about 38% in case of Beam 3 which break down owing to fracture of CFRP. Beam four failed at the termination point due to delamination of the outer CFRP, while concrete cover delamination was observed in case of Beam 5. It was concluded that in bond behavior the thickness and shear modulus of the bond layer is critical. To prevent premature failure, controlling the thickness is important.

Xiao.J et al. (2004) performed a double-shear test and the bending test to evaluate the bond behavior among the FRP and concrete. For the first test (double shear) Concrete specimen was prepared to have a typical strength of 36.1 MPa for 150 x 150 x 150 mm^3 specimen. E-glass composite fibre with the tensile strength 640 MPa, elastic modulus 30 GPa, 30 mm wide was used. Surface preparation was done by an electric grinding wheel. The test result showed that with the increase in load strain in FRP also increased concurrently. Towards the end of loading Local debonding took place in the 115 mm long part. Since there was a remarkable variation of the bond strains over a short range of 50 mm from the makeup the crack, therefore the effective bond length was concluded to be about 100 mm. There was non-uniform bond stress dispersal in the FRP plate with a mean value of 1.287 MPa.

For the Bending type test Two T beams, B-1with continued loading and B-2 without continued loading were tested. FRP used and the surface preparation was done in the same manner as in the previous test, with only difference in the width of the FRP (50 mm). From the test, it was concluded that the development length is about 300 mm for the flexural bond in the

negative moment zone signifying that for the flexural bond length of development is three times of the effective bond length.

Yao et al. (2005) performed an experimental investigation on FRP concrete bonded joints through the adoption of a near end single shear test of a total of 72 samples. Bond length, the ratio of width between the attached FRP and concrete block, the height of the free edge of the concrete, and the angle of load were the test variables chosen for this experiment. For 56 of the 72 specimens failure occurred in the concrete just below the epoxy concrete boundary. Cracking began at the loading end which triggered the debonding and it progressed to the far end before the occurrence of complete debonding. Aggregates were completely visible by looking at the failure surface. Both the positive and negative loading angle had a major influence on the bond strength for bond length of less than 95 mm. For the larger bond length angle of loading becomes insignificant owing it to the angle becoming smaller and smaller during the progression of debonding.

Mazzotti et al. (2008) performed an experimental study by conducting a single shear test to assess the delamination of FRP plates bonded to the concrete. Test variables were the bonded length (50, 100, 200 and 400 mm) and the breadth of the FRP chosen was 50 mm and 80 mm. Concrete specimens with dimensions 150 x 200 x 600 mm were prepared and CFRP used was of thickness 1.2 mm. For Setup A, the bond length of the plate starts right from the corner of the specimen. For Setup B, the bond length of the plate starts 100 mm away from the corner of the specimen. Shearing of concrete having a thickness of 1 to 2 mm was the major failure for all of the specimens. Under the whole plate, Uniform concrete thickness was attached to the adhesive. Maximum anchorage force transmitted by the 50 mm and 80 mm width CFRP were 22.8 kN and 36.2 kN. For Setup A, delamination was of fragile nature even for the long bond length. For the FRP with the smallest bond length that is 50 mm, delamination load for Setup A was sixty percent less as compared to Setup B.

Julio C. et al. (2012) performed an experiment to assess the impact of adhesive thickness and strength of concrete on the outcomes of the beam-type FRP test. The experimental setup consisted of 30 beam-type specimens, strengthened with 1.2 mm thick and 50 mm wide pultruded prefabricated FRP plates bonded with an epoxy adhesive. Before applying the adhesive the surface was chipped. The failure observed was a concrete failure, failure at the interfaces of concrete adhesive along with FRP adhesive and the transverse adhesive failure.

Both the concrete strength and adhesive thickness influenced the ultimate load but in the case of adhesive thickness, the influence was not consistent. Experimental outcomes showed that the failure occurred in the weakest component for low strength concrete it was concrete, while it was concrete – adhesive interface in cases of high strength concrete. The adhesive thickness would play a more important role for high strength concrete, increasing the thickness would promote stress redistribution and increase the ultimate load.

2.2 BOND BEHAVIOUR OF EXTERNALLY BONDED FRP WITH CONCRETE SUBJECTED TO ELEVATED TEMPERATURES

Klamer et al. (2006) performed an experiment to investigate temperature influence on Externally Bonded CFRP debonding. To accomplish these two different test types were used, double shear test and bending type test. Test variables were the Concrete denoted with Series A, B, C and D having different compressive strength (37.7 MPa, 31.5 MPa, 18.6 MPa, and 24.4 MPa) and Temperature varying from -10°C to 75°C. CFRP sheet used had 2800 MPa Tensile Strength, 165000 MPa Elastic modulus, 0.3×10^{-6} / °C coefficient of thermal expansion and temperature resistance till at least 150°C. The adhesive had a 62°C glass transition temperature (*Tg*). For the purpose of surface preparation, sandblasting was used. For the high-temperature heating of specimens for at least 12 hrs in the oven was carried out while for the low temperatures specimens were frozen for at least 24 hrs. From the Double lap shear test results it was observed that for the moderate temperature (20°C and 40°C) breakdown occurred in the concrete while for the elevated temperatures (50°C, 65°C and 75°C) occurrence of debonding at the concrete adhesive interface was observed. For the low temperature (50°C) failure was similar to the 20°C specimen. For the high temperatures (65°C and 75°C) decrease in failure load was also observed. Similar failure was observed in the bending type test also. The adhesive strength was highly decreased particularly for the temperature greater than the glass transition temperature.

Leone et al. (2009) performed experimental research to evaluate the Effect of elevated temperature on FRP concrete bond. To accomplish this double shear test was executed on a total of 18 specimens (150 x 150 x 400 mm) varying the temperature. Test variables were type of FRP (wet lay-up sheet or factory made), fibre type (CFRP sheet and laminate, GFRP sheet) and temperature (50°C, 65°Cand 80°C). The adhesive used had a glass transition temperature (*Tg*) of 55°C. From the test result, higher bond stress was obtained for the CFRP laminates owing to the better quality control in manufacturing. With the rise in temperature bond stress decreased

especially for the temperature greater than adhesive's glass transition temperature (*Tg*). For a particular temperature (80°C) the decrease in bond stress for CFRP sheet, GFRP sheet, and CFRP laminate was 54%, 72%, 25% respectively in comparison to room temperature. With the rising temperature, the type of failure changed. Failure within the concrete was observed for specimens tested at 50 °C while the interface failure was observed for specimens tested at 80°C.

Haddad et al. (2013) conducted a double shear test to examine the influence of elevated temperature on the bond among the CFRP sheets and lightweight concrete, normal weight concrete. Concrete Specimen made from NWAC and LWAC having dimensions of 150 x 150 x 100 mm were subjected to temperatures extending from 300°C to 600°C. CFRP sheets used were having width varying (50, 100 and 150 mm), 0.17 mm thickness, 3600 MPa Tensile Strength and a connected length of 100 mm. Before the CFRP sheets were bonded with specimen the surface preparation was done with the help grinding disk. Debonding in concrete neighboring to concrete adhesive boundary lead to the failure of the majority of the specimen. With the escalation of temperature, the peeling width and the concrete peeling depth also increased. Temperatures more than 500 °C lead to the debonding of the unbonded top fraction of the specimen owing to the decrease in shear strength with the rise in temperature. For the Specimen exposed to temperatures higher than 400°C bond strength was reduced to 64 %. While the slip at failure increased 254% of control values respectively. For temperatures higher than 400°C LWAC specimens displayed low peel off depth and breadth as compared to NWAC of comparable strength.

Danie Roy et al. (2015) performed an experiment to determine the impact of high temperatures on FRP concrete bond quality. Single shear pull off test was done on 45 specimens (150 mm x 150 mm x 300 mm), which were casted heated and bonded GFRP unidirectional fiber sheets with 0.324 mm thickness and 3400 MPa tensile strength. Test variables were the temperature (Ambient, 200°C, 400°C, 600°C, 800°C) and the bond length (100 mm, 150 mm, 200 mm). Specimens were heated at the pace of 10°C/min and to achieve thermal steady state condition each of the target temperatures was sustained for 3 hours. Before bonding with GFRP laminate the specimens were allowed to cool off for 24 hrs after switching off the furnace. Surface preparation was done by hand grinding until the aggregates become clear. Thirty specimens failed by debonding of the concrete where the thickness of concrete layer getting detached was 4- 25 mm, while the rest of the specimens failed by debonding at the concrete adhesive boundary with the thickness of concrete layer getting detached was less than 4 mm.

Time of debonding failure was dependent on the bond length, was small for short bond length and large for longer bond length. From the Load vs Slip curve, it was observed that the slip was linear up to 400°C, while for temperature above 400°C it was nonlinear even in the early stages of loading. It was also noted from the outcomes that the debonding always began at the loaded end. The longer bond length also resulted in increased bond strength. This study was further taken for Finite Element Modelling.

2.3 BOND RELATED ANALYTICAL MODELS

Across the research community of FRP Strengthening, it is recognized that there is an effective bond area through which most interfacial shear forces are transmitted from the fibre layer to the concrete. This region of length is defined as the effective bond length, which is the length over which the failure load ceases to increase and the strain in FRP disappears and is FRP width dependent. Various models were established on empirical information and theories of fracture mechanics, some of which were additionally modified for design usage. The overview of the efficient bond length as indicated by different FRP codes is shown in Table 2.1

Table 2.1 Summary of the effective bond length (Ouezdou, M.B, et al.2009)

Code	Year	Expression	Reference applied
ACI 440.2R-02[1] (*USA*)	2002	$L_e = \frac{23300}{(nE_f t_f)^{0.58}}$	Maeda et al.[9] $L_e = e^{6.134 - 0.58\ln(E_f t_f)}$
ISIS[2] CSA S806-02[3] *(Canada)*	2002	$L_e = \frac{25350}{(E_f t_f)^{0.58}}$	Maeda et al.[9] $L_e = e^{6.134 - 0.58\ln(E_f t_f)}$
FIB B14[4] –Appendix A1 (*Europe*)	2001	$L_e = \sqrt{\frac{E_f t_f}{c_2 f_{ctm}}} \quad c_2 = 2$	Neubauer and Rostásy[10] $L_e = \sqrt{\frac{E_f t_f}{2 f_{ctm}}}$
FIB B14[4] - Appendix A2 *(Europe)*	2001	$L_e = c_2\sqrt{\frac{E_f t_f}{f_{ck} f_{ctm}}} \quad c_2 = 1.44$	-
CS TR55[5] (*UK*)	2004	$L_e = 0.7\sqrt{\frac{E_f t_f}{f_{ctm}}}$	Neubauer and Rostásy[10] $L_e = \sqrt{\frac{E_f t_f}{2 f_{ctm}}}$
CNR-DT 200/04[6] (*Italy*)	2005	$L_e = \sqrt{\frac{E_f t_f}{2 f_{ctm}}}$	FIB- B14 - Apx A1[4] $L_e = \sqrt{\frac{E_f t_f}{c_2 f_{ctm}}} \quad c_2 = 2$
Eurocode 8-3[7](*Europe*)	2004	$L_e = \sqrt{\frac{E_f t_f}{4 f_{ctm}}}$	-
CIDAR[8](*Australia*)	2006	$L_e = \sqrt{\frac{E_f t_f}{\sqrt{f_c'}}}$	Chen and Teng[11] $L_e = \sqrt{\frac{E_f t_f}{\sqrt{f_c'}}}$

E_f = elastic modulus of FRP, L_e = effective bond length, f_c' = concrete strength, f_{ck} = characteristic strength of concrete, f_{ctm} = mean tensile strength of concrete, n = number of layers of FRP, t_f = thickness of FRP, τ_{max} = maximum bond strength of FRP onto concrete surface

If we take into account theoretically then bonded lengths beyond the effective bond length would be ineffective as the FRP's full strength should have been already exceeded. Still, bond lengths are required much higher than the efficient bond length as it leads to more ductile failures by allowing localized debonding and the active zone to shift away from the cracking zone.

Several Bond Strength models were suggested for the bond strength between FRP sheet/laminates and concrete together with Bond Length Models. Few of the models were established on empirical relations which were assessed with experimental information as in the case of Tanaka 1996, Hiroyuki and Wu 1997 and Maeda et al. 1997. Some other models have established on fracture mechanics theories, with different factors been evaluated with experimental information as in case of Holzenkämpfer 1994, Täljsten 1994, Niedermeier 1996, Neubauer and Rostásy 1997, Blaschko et al. 1998, Yuan and Wu 1999, Yuan et al.2001. Using basic assumptions design models were also prepared which were then verified against experimental data as in case of Van Gemert 1980, Sato et al.1997, Challal et al. 1998, Khalifa et al. 1998, Izumo et al. 1999, Sato et al. 2001, Chen and Teng 2001 and JCI 2003. For all the models, Single Shear test is used to simulate the stress behavior on a sample bonded with FRP plate. Table 2.2 summarizes various Bond Strength Models.

Table 2.2 Bond Strength Models (Sayed-Ahmed et al. 2009)

Model Name	Model
Hiroyuki and Wu Model (Hiroyuki and Wu 1997)	$\tau_u = 0.27 \cdot L^{-0.669}$ $P_u = \tau_u \cdot L \cdot b_p$
Tanaka Model (Tanaka 1996; Sato et al. 1996)	$\tau_u = 6.13 - \ln(L)$ $P_u = \tau_u \cdot L \cdot b_p$
Maeda Model (Maeda *et al.* 1997)	$\tau_u = \left(110.2 \times 10^{-6}\right) E_p t$ $P_u = \tau_u L_e b_p \qquad L_e = e^{2.1235 - 0.580 \cdot \ln(E_p t_p)}$
Khalifa *et al.* Model (Khalifa *et al.* 1998)	$\tau_u = \left(110.2 \times 10^{-6}\right)\left(f_c' / 42\right) \cdot E_p t_p$ $P_u = \tau_u L_e b_p \qquad L_e = e^{2.1235 - 0.580 \cdot \ln(E_p t_p)}$

Sato Model (Sato *et al.* 2001; Sato *et al.*1997; JCI 2003)	$\tau_u = 2.68x10^{-5}\left(f_c'\right)^{0.2} E_p t_p$ $P_u = \tau_u L_e \left(b_p + 7.4\right)$ $L_e = 1.89\left(E_p t_p\right)^{0.4} \quad if\ L > L_e : L_e = L$
Iso's Model (JCI 2003)	$\tau_u = 0.93\left(f_c'\right)^{0.44} \qquad P_u = \tau_u L_e b_p$ $L_e = 0.125\left(E_p t_p\right)^{0.57} \quad if\ L > L_e : L_e = L$
Yang Model (Yang *et al.* 2001)	$P_u = \left(0.5 + 0.08\sqrt{0.01\, E_p t_p / f_t}\right) \cdot b_b L_e \tau_u$ $L_e = 100\ mm \qquad \tau_u = 0.5 \cdot f_t$
Izumo Model (Izumo *et al.* 1999; JCI 2003)	$CFRP: P_u = \left(3.8 f_c'^{0.67} + 15.2\right) L\, E_p b_p t_p$ $AFRP: P_u = \left(3.4 f_c'^{0.67} + 69\right) L\, E_p b_p t_p$
Chen and Teng Model (Chen and Teng 2001)	$P_u = 0.427 \beta_p \beta_L \sqrt{f_c'} L_e \quad L_e = \sqrt{E_p t_p / \sqrt{f_c'}}$ $\beta_p = \left[\frac{2 - \left(b_p / b_c\right)}{1 + \left(b_p / b_c\right)}\right]^{0.5} \quad \beta_L = \begin{cases} 1 & L \geq L_e \\ \sin\left(\frac{\pi L}{2L_e}\right) & L < L_e \end{cases}$
Holzenkämpfer Model (Holzenkämpfer 1994; Niedermeier 1996; Blaschko *et al.* 1998)	$P_u = \begin{cases} 0.78 b_p \sqrt{2 G_f E_p t_p} & L \geq L_e \\ 0.78 b_p \sqrt{2 G_f E_p t_p} \cdot \alpha & L < L_e \end{cases}$ $\alpha = \left(\frac{L}{L_e}\right)\left(2 - \frac{L}{L_e}\right) \qquad L_e = \sqrt{\frac{E_p t_p}{4 f_t}}$ $G_f = c_f f_t k_p^2 \quad k_p = \sqrt{1.125\left(\frac{2 - b_p / b_c}{1 + b_p / 400}\right)}$
Täljsten Model (Täljsten 1994)	$P_u = b_b \sqrt{\frac{2 G_f E_p t_p}{1 + \left(E_p t_p / E_c t_c\right)}}$
Yuan and Wu Model (Yuan and Wu 1999)	$P_u = b_b \sqrt{\frac{2 G_f E_p t_p}{1 + \left(E_p t_p b_b / E_c t_c b_c\right)}}$
Neubauer and Rostásy Model (Neubauer and Rostásy 1997)	$P_u = \begin{cases} 0.64 k_p b_p \sqrt{E_p t_p f_t} & L \geq L_e \\ 0.64 k_p b_p \sqrt{E_p t_p f_t} \cdot \alpha & L < L_e \end{cases}$ $\alpha = \left(\frac{L}{L_e}\right)\left(2 - \frac{L}{L_e}\right) \quad L_e = \sqrt{\frac{E_p t_p}{2 f_t}} \quad G_f = c_f f_t$

Neubauer and Rostásy Model (Neubauer and Rostásy 1997)	$P_u = \begin{cases} 0.64 k_p b_p \sqrt{E_p t_p f_t} & L \geq L_e \\ 0.64 k_p b_p \sqrt{E_p t_p f_t} \cdot \alpha & L < L_e \end{cases}$ $\alpha = \left(\frac{L}{L_e}\right)\left(2 - \frac{L}{L_e}\right) \quad L_e = \sqrt{\frac{E_p t_p}{2 f_t}} \quad G_f = c_f f_t$
van Gemert Model (van Gemert 1980)	$P_u = 0.5 \cdot b_p \cdot L \cdot f_t$
Challal *et al.* Model (Challal *et al.* 1998)	$\tau_u = 0.5\, \tau_{\max}^{debonding} = 2.7/(1 + k_1 \tan 33^o)$ $k_1 = t_p \left(E_a b_a / 4 E_p I_p t_a\right)^{0.25}$
Where, b_c is the concrete section width, b_p is the width of the bonded FRP plate (mm), b_a is the width of the adhesive, c_f is a constant determined from a regression analysis of FRP pull test, E_p is the modulus of elasticity of the bonded FRP plate (MPa), E_a is the modulus of elasticity the adhesive, f'_c is the concrete compressive strength (MPa), f_t is the concrete surface tensile strength determined in a pull-off test according to DIN 1048, G_f is the fracture energy, k_p is a geometric factor related to the widths of the concrete and the bonded FRP plate, L is the bonded length (mm), L_e is the effective bond length (mm), I_p is the second moment of area of the FRP plate, P_u is the bond strength of a joint (N), t_a is the thickness of the adhesive, t_p is thickness of the bonded FRP plate (mm), β_L is a geometric bond length coefficient, β_P is a geometric width coefficient, τ_u is the ultimate shear stress (MPa), and τ_f and δ_l are the maximum shear stress and corresponding slip on the shear stress-slip (bond-slip) curve with a maximum slip of δ_f.	

2.4 FINITE ELEMENT MODELS

Current Finite element research on the FRP to concrete bonded joint as discussed for subsequent literature can be categorized into three approaches:-

- Direct modeling approach: A mesoscale finite element mesh with the minutest size of the element size frequently in the confines of 0.5 mm to 2 mm is used in the direct modeling method to model the precise behavior of concrete adjacent the FRP concrete bond line such that the bond slip behavior could be achieved.
- Interface modeling approach: The layers of interface elements are used in this technique to mimic the bond conduct. The interface model method is most frequently employed for modeling reinforced FRP systems or for modeling three-dimensional conduct because, owing to high computing requirements, designing the entire reinforced 3D structure using

mesoscale components is unrealistic. Interface elements of zero thickness are normally employed to represent the FRP concrete boundary.

- Crack band modeling approach: This strategy implies that debonding happens in the concrete close to the adhesive to concrete boundary within a narrow range, and the characteristics of the concrete within this group differ from the neighboring plain concrete due to adhesive admittance.

Ibrahim and Mahmood (2009) performed finite element modeling of reinforced concrete beams externally enhanced with FRP laminates. ANSYS was used for the analysis of six beams. The findings acquired from the analysis were associated with the literature experimental information. To model reinforced concrete smeared cracking approach was used. Element used for modeling of the concrete was Solid 65. Various parameters of concrete which were entered in ANSYS were: ultimate tensile strength, ultimate compressive strength, modulus of elasticity, shear transfer coefficient, Poisson's ratio and stress-strain relation of concrete. For the modeling of steel reinforcement element type Link, 8 was used. Yield stress, elastic modulus, and Poisson's ratio were the characteristics of the steel reinforcement which were entered in ANSYS. For the modeling of FRP composites layered element type Solid 46 was used. As the concrete beam was symmetrical in cross-section and loading, the finite element analysis was done by modeling of only one-fourth of the beam. This considerably decreased the demands for computing time and computer disk space.

Through the full range of behavior and failure mode, the load deflection values acquired from the ANSYS showed excellent consistency with the experimental outcomes. Finite element model for all the beams was firmer than the actual beam in the linear region. It was also observed that the FRP enhanced beams were stiffer than the unreinforced beams, with a better performance of carbon fiber polymer than the glass fiber polymer. Also with the FRP strengthening of the beam failure was shifted from the shear failure at the ends to flexure failure at the midspan.

Chen and Tao (2011) performed Finite Element Modelling of Pull off/single shear test in ABAQUS for replicating the FRP Concrete bond conduct. For the modeling of concrete smeared cracking method was employed as it is difficult to record numerous cracks, particularly the different micro cracks in the single shear test where the concrete neighboring to the FRP fails within a few mm. For the FE analysis Concrete prism of 45 mm thickness was formed as a plane

stress issue. Finite Element Model used size was lower than the samples used in the studies, but since the debonding arise in concrete a few mm away from the concrete FRP interface, the concrete residue would not have a significant impact. As shown in the above Figure, the sample was restricted vertically and horizontally. Elastic moduls of the FRP Plate was altered in order to keep the stiffness same as the thickness of the plate was kept 1 mm. Width ratio factor β was proposed by Chen & Teng (2001) was used to attune the results from the analysis as it was formed as a plan stress issue while the actual behaviour being three dimensional.

$$\beta_w = \sqrt{\frac{2 - b_f / b_c}{1 + b_f / b_c}}$$

Where b_f represents the FRP Plate's Width and b_c represents the concrete prism width respectively. Load vs slip curve assessment between the experimental data and the Finite element model data for one of the specimens showed that the FE predictions are in close contact with test data for the entire loading range.

Mohamed and Khattab (2016) performed finite element modeling of FRP sheets attached externally to the concrete. ANSYS was used to simulate the double shear test behavior. The finite element model findings were contrasted with the two codes, i.e. American code and Italian code. Concrete was modeled using Solid65 element due to its ability to crush in compression and crack in tension. Cracking was modeled using the smeared crack approach. For modeling of the reinforcing bars, LINK180 element was used whereas for the modeling of the FRP Sheets Solid45 element was used. The epoxy layer between the FRP and concrete was modeled using a contact element. Properties used for determining the effective bond length and strain using American and Italian code was: concrete compressive strength *fc*, concrete elastic modulus E_c, FRP elastic modulus E_f and thickness of the FRP t_o. The strain was maximum at the first contact point between the two concrete prisms and diminishes away from the centerline. From the results, it was seen that the two codes American and Italian offer conservative estimates of effective bond length while only American code was conservative in the estimation of maximum strain.

Mabroukand Ramadan (2017) performed a finite element modeling of a reinforced concrete beam enhanced by CFRP sheet externally bonded in shear. For this purpose ABAQUS was used. Concrete damage plasticity model inbuilt in the ABAQUS was used to depict the Non-Linear behaviour of the concrete. For the modeling of the concrete element, C3D8R was used whereas

Truss element T3D2 was used for modeling of steel bars. Embedded interaction technique in ABAQUS was used for the simulation of the bond between steel and concrete. This interaction allows for approximate bond stress-slip constitutive model and transfers tension force from concrete to steel across cracks. FRP sheets were molded using linear elastic behavior up to de-bonding from the concrete substrate. Shell element S4R was used to model FRP. Since the beam was symmetrical along with the loading, modeling of only one-fourth of the beam was done to save the analysis time. CFRP sheets bonded on the web of the beam were 50 mm wide, 1.2 mm thick, with 100 mm c/c spacing and modulus of elasticity being 165 GPa. Results indicated that the FRP plates boosted the beam's shear ability by about 23 percent and the beam ductility improved by about 50 percent relative to the shear failure control beam. Finite Element Modelling data is closely aligned with the experimental data.

CHAPTER 3

FINITE ELEMENT MODELING

In this chapter Finite Element Modelling of Heat damage concrete specimen externally bonded with GFRP laminate is presented. The Geometrical Properties, Material Characteristics, Boundary conditions as well as the loading settings were taken from the experimental research which was performed by Danie Roy et al. (2015). For this purpose commercial available software ANSYS Workbench15.0 is used.

ANSYS Workbench is a simulation tool that allows customers to use the FEA to model and address a broad variety of engineering issues. It offers access in an embedded simulation setting to the ANSYS family of design and assessment modules. ANSYS Workbench essentially provides access to ANSYS applications with tools that handle the workflow of the product. A schematic workflow, which handles the links between the systems, drives the project.

In a typical ANSYS analysis, there are three primary steps:

1. **Generation of a Model:**
   - Idealizations and Simplifications of the problem.
   - Defining the characteristics of the respective material.
   - Generation of the finite element model or meshing.
2. **Solution:**
   - Specifying the loading circumstances and boundary conditions.
   - Achieving a solution.
3. **Reviewing the outcomes or results:**
   - Plotting or listing of the results.
   - Checking for legitimacy or validity.

All of the above steps refer to a particular processor or processors within the ANSYS processing unit. Model generation is carried out generally in the preprocessor whereas the appliance of the loading and the solution is carried out in the solution processing unit. Finally, the outcomes are considered for static (static) and temporary (time-dependent) issues respectively in the General Postprocessor and Time History Postprocessor.

3.1 ANALYSIS SYSTEM

Analysis System used in ANSYS workbench for simulation was Static Structural Analysis as depicted in Figure 3.1

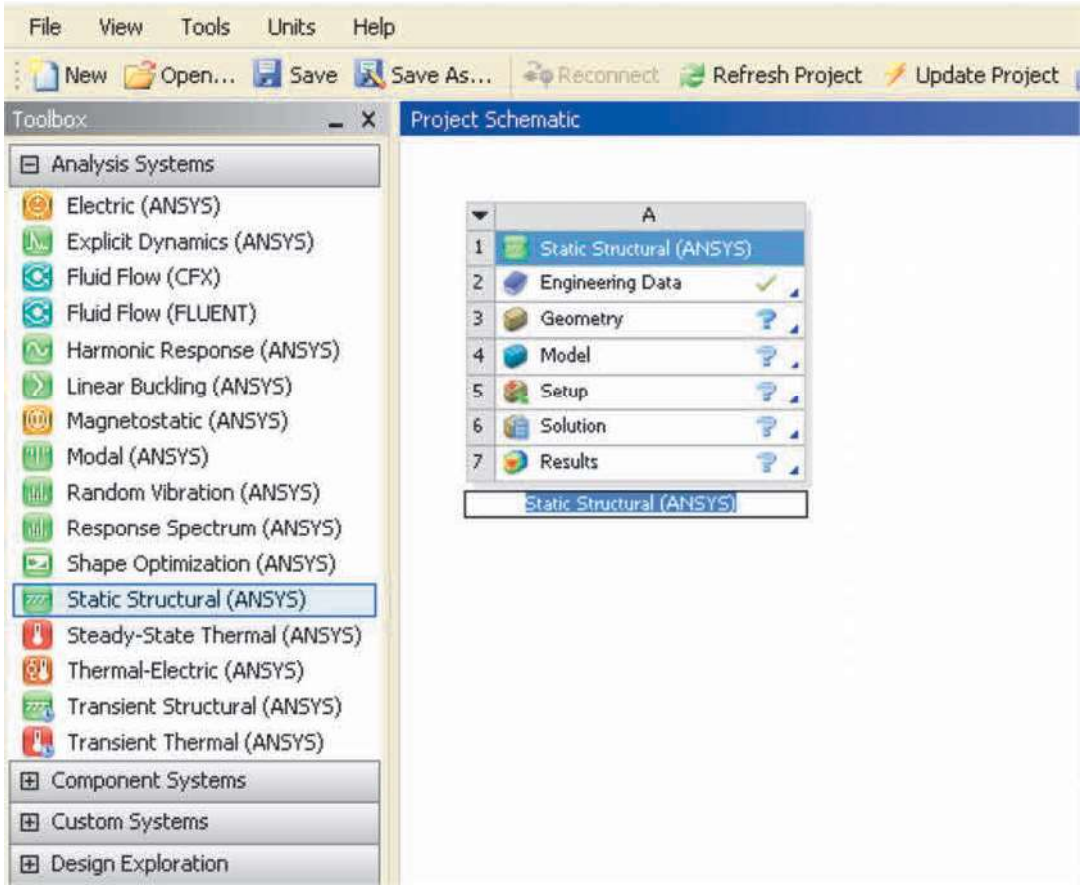

Figure 3.1 ANSYS Workbench Project Mode

A static structural analysis figures the forces, stresses, displacements, and strains induced by loads in buildings or elements that do not cause important impacts of inertia and damping. Stable conditions of loading and feedback is assumed; that is the loads and the response of the structure are assumed to vary slowly over time. Whichever system is placed on the Project Schematic comprises of analysis components called cells as shown in Figure 3.1. Cells are essentially the components that make up a system of analysis.

The following list includes the cell kinds and their expected features accessible in ANSYS Workbench:

- **Engineering Data** deals with the defining or editing of material properties of the model to be used in an analysis.

- **Geometry** deals with the Creation, importing or editing of the geometry model to be used for analysis. In our case geometry was created in **SOLID WORKS** and was imported as a Step File in ANSYS Workbench.
- **Model/Mesh** deals with the assigning of the material, defining the coordinate system, and generating the meshing for the model.
- **Setup** deals with the application of the loads, defining the boundary conditions, and configuration of the analysis settings.
- **The solution** deals with accessing the model solution or sharing of the data with other systems.
- **Results** Specify the accessibility and status of outcomes which also referred to as post-processing).

3.2 MODELING OF THE SPECIMEN

3.2.1 Assumptions

The assumptions taken in the specimen's FEM modeling are outlined below:-

- Concrete is modeled as homogeneous and isotropic material.
- GFRP is modeled as an orthotropic material
- The FRP carries stress along its axis only.

3.2.2 Failure Criteria of The Concrete

The nonlinear concrete model in ANSYS is centered on the William and Warnke failure criteria. According to the failure criteria of William and Warnke, at least two strength parameters are required to describe concrete's failure surface. When the failure exceeds crushing of the concrete will occur if principal stresses are tensile else crushing of the concrete will occur if all the principal stresses are compressive. Tensile failure comprises of a benchmark for maximum tensile stress. The material behavior is linearly elastic until failure unless plastic deformation is taken into consideration.

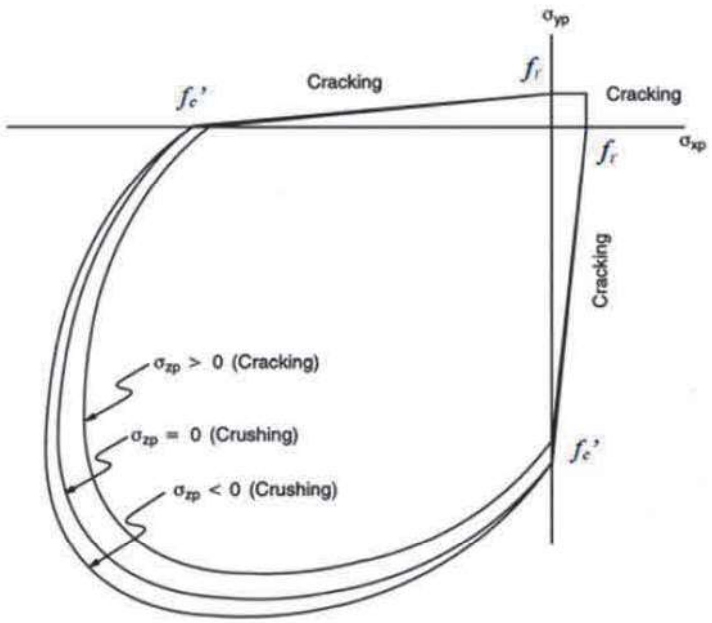

Figure 3.2 Concrete's Three dimensional Failure Surface (SAS, 16.2)

Figure 3.2 depicts the Concrete's Three-dimensional Failure Surface. The utmost important non-zero principal stresses are in both the x direction and y-direction, denoted by σ_{xp} and σ_{yp} respectively. On the σ_{xp}- σ_{yp} plane three failure surfaces are shown as the projections. The failure modes are the function of the sign of principal stress in the Z direction which is denoted by σ_{zp}. For instance, if σ_{xp} and σ_{yp}, both are negative meaning compression and σ_{zp} is slightly positive meaning tension then cracking would be anticipated in a direction at a right angle to σ_{zp}. But, if σ_{zp} is zero or to some degree negative, then the material is expected to crush. Cracking happens in a concrete component when the principal stress is in tension and beyond the failure surface in any direction. After splitting, the concrete element's elastic modulus is set to zero in the direction parallel to the principal tensile stress direction. Similarly when all principal stresses are compression and lie beyond the failure surface Crushing in concrete will occur. Subsequently, in all directions, the elastic modulus is set to zero and the component disappears effectively.

3.2.3 FRP's Failure Criteria

FRP composite is not a homogeneous material. Their characteristics depend on many variables, the most significant of which are fiber type, fiber amount (as a percentage of volume) and the direction of their placement. The FRP composite is usually fully elastic up to breakdown and display no yield point or plasticity section. They are likely to have minor strain to failure, generally less than three percent. If all the fibers are arranged in one direction, the compound is

comparatively rigid and strong in that particular direction, but it has small modulus and poor strength in the crosswise direction. Failure of the unidirectional FRP is mainly influenced by the tensile strength in the longitudinal direction and the lengthening at breakage.

3.2.4 Single Shear Experimental Test Setup

Figure 3.3 depicts the Single Shear Test Setup of an experimental study done by Danie Roy et al.2015.

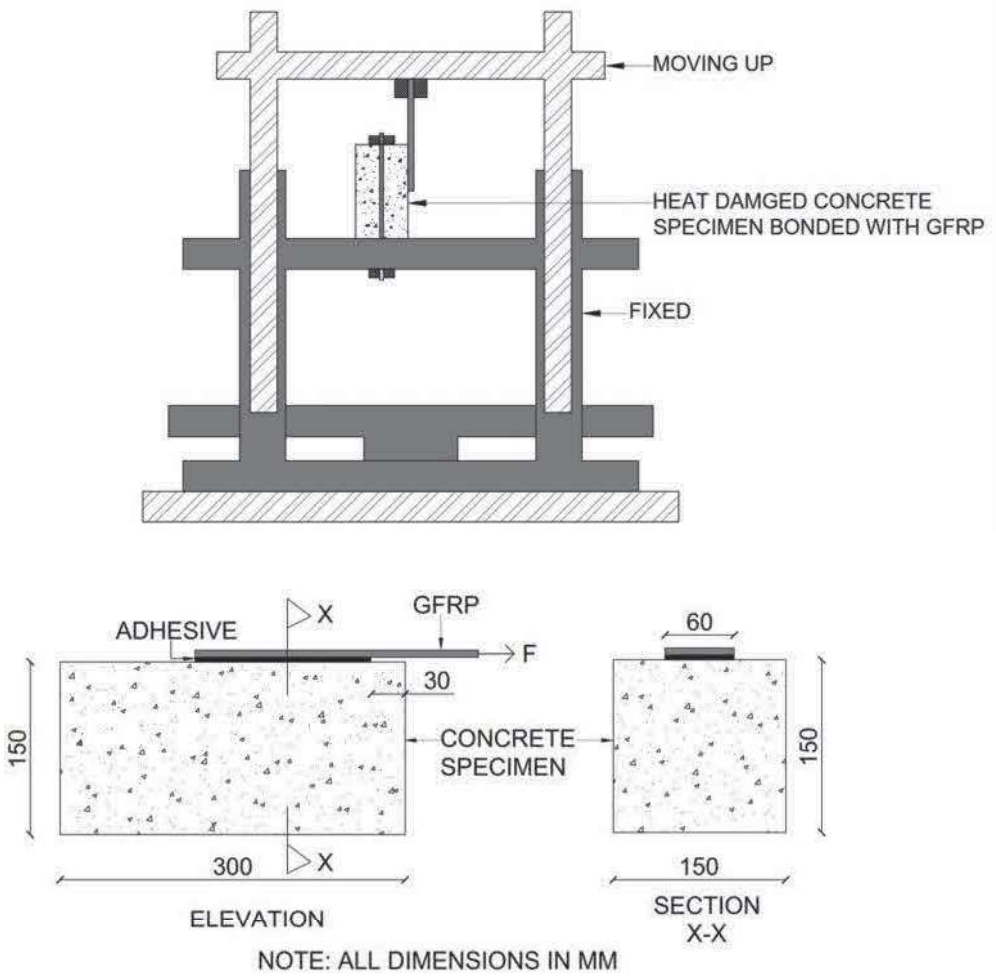

Figure 3.3 Single Shear Test Setup (Danie Roy et al. 2015)

3.2.5 Element Type

The Solid187 element type is used to form the Concrete and FRP model. SOLID187 element is a higher order three dimensional ten noded elements which has a quadratic displacement behavior. The element is characterized by ten nodes having three degrees of freedom at each node which are translations in the nodal x, y and z directions. The element has

stress stiffening, creep, plasticity, hyperelasticity, large deflection, and large strain proficiencies. Figure 3.4 shows the representation of the element SOLID187.

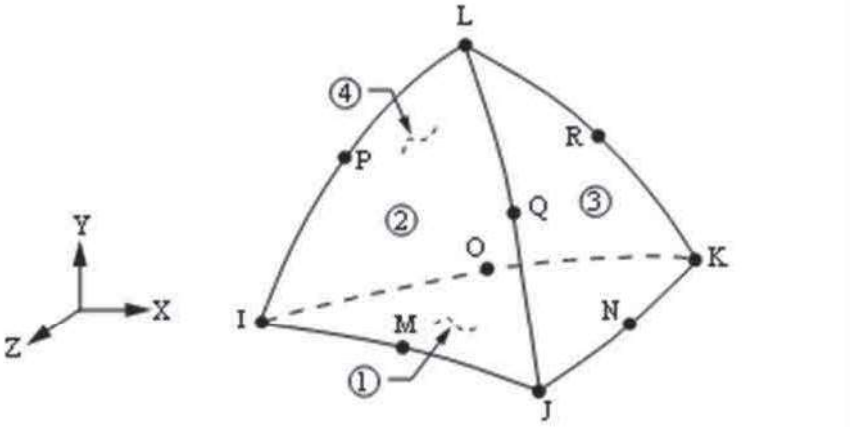

Figure 3.4 Solid 187 Element (SAS, 16.2)

For contact between FRP and Concrete, CONTA174 Element is used**.** Figure 3.5 depicts a schematic of the element CONTA174.

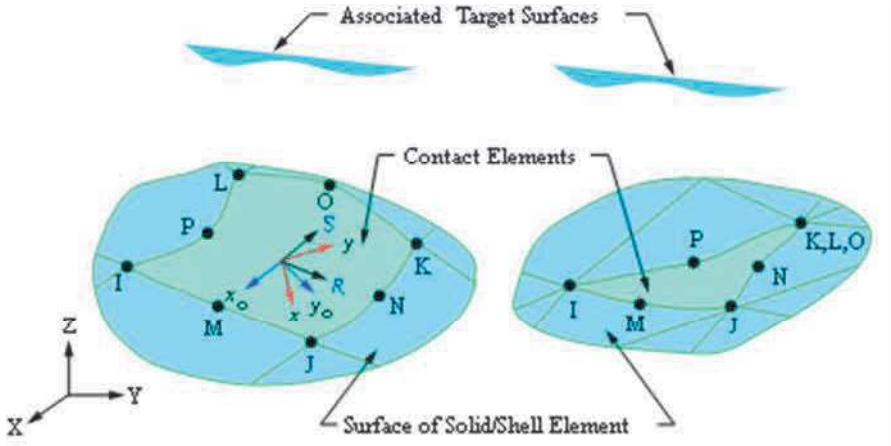

Figure 3.5 Element CONTA174 (SAS, 16.2)

CONTA174 is used to depict contact as well as sliding between three-dimensional target surfaces and a deformable surface that this component defines. The element is applicable to three-dimensional structural analysis and coupled field contact analysis. For both general contact and pair-based contact, CONTA174 can be used. For the pair based contact three-dimensional target element TARGE170, is used to define the target surface. The element is located on the surfaces of three dimensional solid or shell elements with midside nodes as in the instance of element Solid187.

For the associated contact element CONTA174, TARGE170 is employed to represent Three-dimensional target surfaces. The contact elements themselves overlay the solid, shell or line elements that describe a deformable body's boundary and are potentially in contact with the target surface as defined in TARGE170. These elements can easily model complex target shapes. Figure 3.6 depicts the schematic of the element TARGE170.

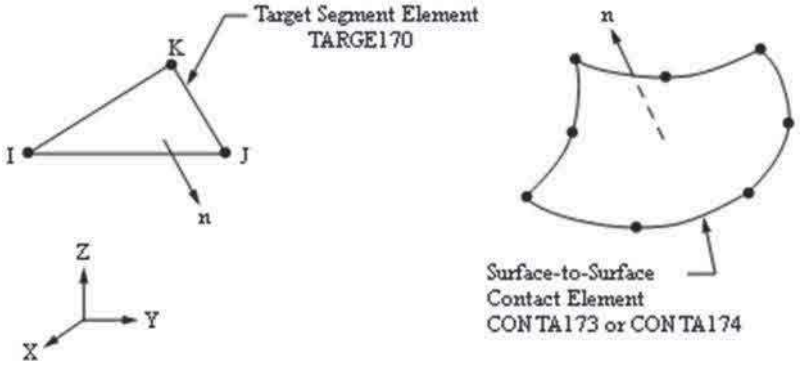

Fig 3.6 Element TARGE170 (SAS, 16.2)

3.2.6 Material Properties

3.2.6.1 *Properties Of Concrete*

Two main characteristics Compressive strength of the concrete and Splitting Tensile strength of the concrete specimens for the various temperatures were obtained from the Literature (**Danie Roy et al. 2015**) and are mentioned in the following Table 3.1

Table 3.1. Concrete Compressive strength and Tensile strength at various temperatures (Danie Roy et al. 2015)

Temperature (°C)	**Concrete Compressive Strength (MPa)**	**Tensile Strength (MPa)**
Ambient(30)	43.75	4.07
200	41.21	3.51
400	35.18	2.87
600	16.46	0.97
800	6.37	0.47

The concrete's modulus of Elasticity taken is established on the equation given below (as per Cl. 6.2.3.1 of IS 456: 2000)

$$Ec = 5000\sqrt{f}$$

Therefore the respective Concrete's modulus of Elasticity was obtained for Concrete specimens at various temperatures.

Poison ratio of the concrete was varied between 0.15 – 0.2

Bulk Modulus and Shear Modulus was automatically calculated by ANSYS Workbench.

The density of the concrete was set to 2400kg/ m^3.

3.2.6.2 *Properties Of GFRP*

Properties of GFRP used in ANSYS Workbench is given in Table 3.2

Table 3.2 GFRP Properties

PROPERTY	VALUE
Type	E — Glass 90/10
Thickness, mm	0.324
Density, g /cm^3	2.75
Tensile strength, Mpa	3400
Young's Modulus X direction, MPa	1.25e+005
Young's Modulus Y direction, MPa	9000
Young's Modulus Z direction, MPa	9000
Poisson's Ratio XY	0.24
Poisson's Ratio YZ	0.46
Poisson's Ratio XZ	0.24
Shear Modulus XY, MPa	30000
Shear Modulus YZ, MPa	1.e-004
Shear Modulus XZ, MPa	1.e-004

3.2.6.3 *Properties Of Epoxy*

Properties of Epoxy used in ANSYS Workbench is mentioned in Table 3.3

Table 3.3 Epoxy Properties

PROPERTY	VALUE
Density, kg /mm^3	2.16e-006
Poisson's Ratio	0.23
Young's Modulus, MPa	723
Shear Modulus, MPa	293.9
Bulk Modulus, MPa	446.3
Critical Fracture Energy for Normal Separation, mJ /mm^2	0.28
Maximum Normal Contact Stress, MPa	1.7
Critical Fracture Energy for Tangential Slip, mJ /mm^2	1.e-033
Maximum Equivalent Tangential Contact Stress, MPa	1.e-036
Artificial Damping Coefficient's	1.e-008

3.2.7 Modeling of Specimens

Concrete Specimens having dimensions (150mm x 150mm x 300 mm), Bonded with GFRP Laminate of 60 mm width with varying bonded length(100 mm, 150 mm and 200 mm). Therefore 3 geometry models were created for three different bonded length in SOLIDWORKS and were exported as a STEP File format. The same Step files were imported in ANSYS Workbench geometry. Figure 3.7, 3.8 and 3.9 shows the Model created in the ANSYS Workbench for 100 mm,150 mm and 200 mm GFRP Bonded Length.

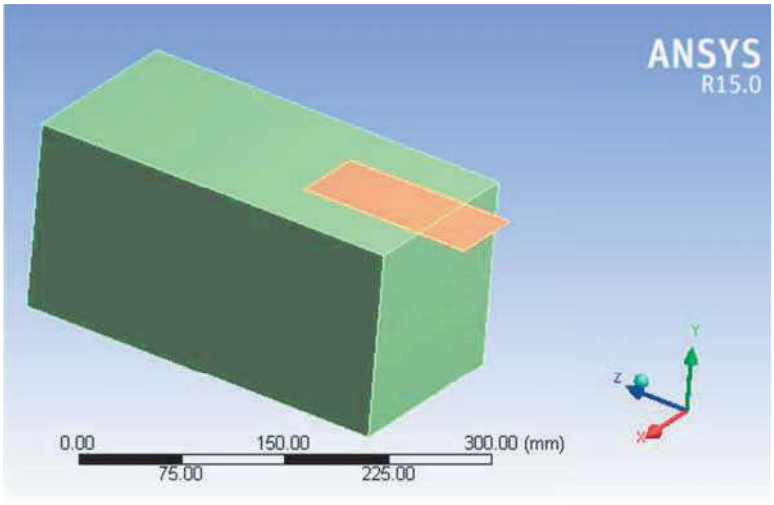

Figure 3.7 Concrete Specimen with Bonded GFRP (100 mm)

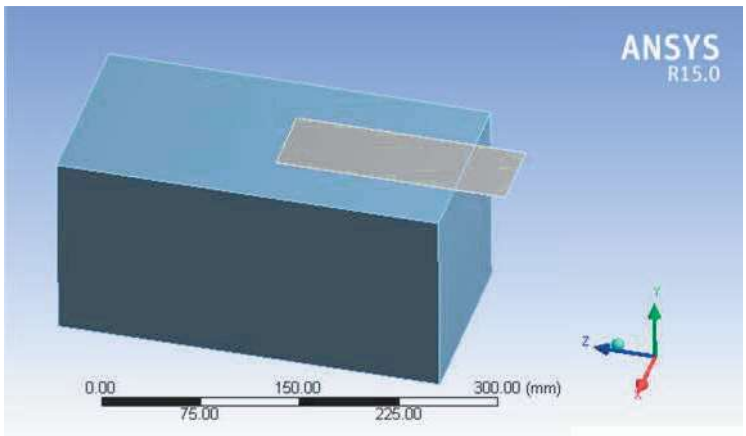

Figure 3.8 Concrete Specimen with Bonded GFRP (150 mm)

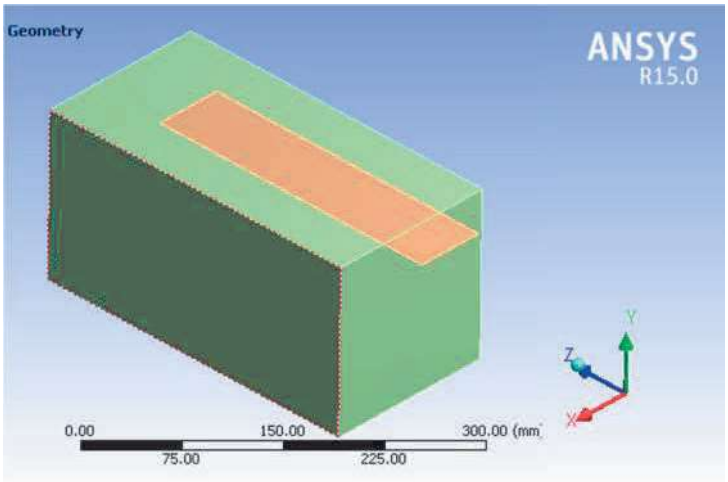

Figure 3.9 Concrete Specimen with Bonded GFRP (200 mm)

3.2.8 Meshing

The use of a triangular mesh is used to achieve better results from the Solid187 element. The mesh is set up to create triangular elements. Figure 3.10 depicts the overall meshing in the ANSYS for the Concrete specimens bonded with GFRP of 200 mm in length. Same way meshing is done for the rest of the specimens also. For the FRP finer Mesh is chosen.

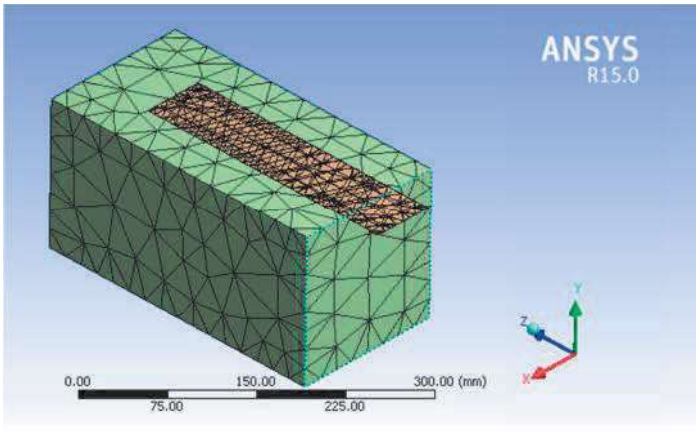

Figure 3.10 Meshing of Concrete Specimen with Bonded GFRP (200 mm)

3.2.9 Loads And Boundary Condition

Finite Element Analysis illustrative view of Load and Boundary Condition is shown in Figure 3.11 The specimen's bottom is held fixed to simulate the experimental behavior. The support condition at the bottom of the Concrete specimen with Bonded GFRP (200 mm) is shown in Figure 3.12. The force F, which is uniformly distributed over the GFRP thickness is applied at the end of the FRP. Figure 3.13 illustrates the applied loading.

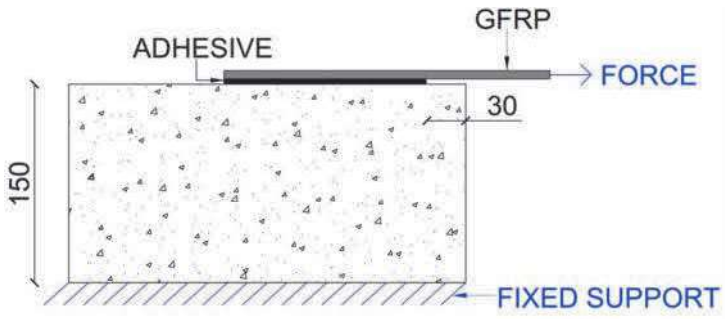

Figure 3.11 Finite Element Analysis illustrative view of Load and Boundary Condition

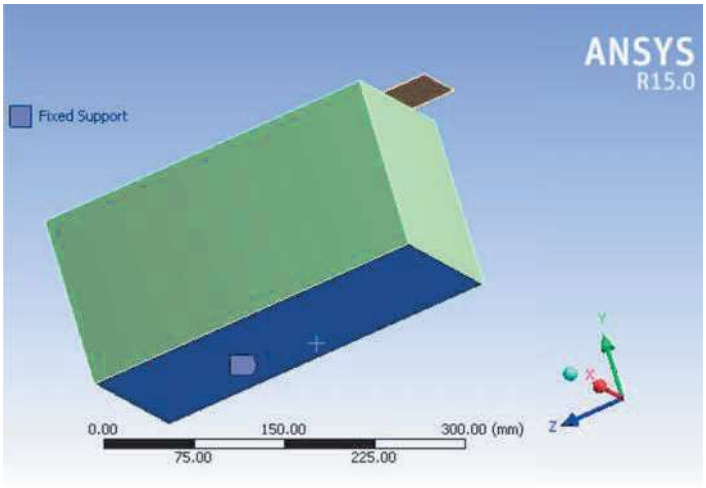

Figure 3.12 Boundary Condition of Concrete Specimen with Bonded GFRP (200 mm)

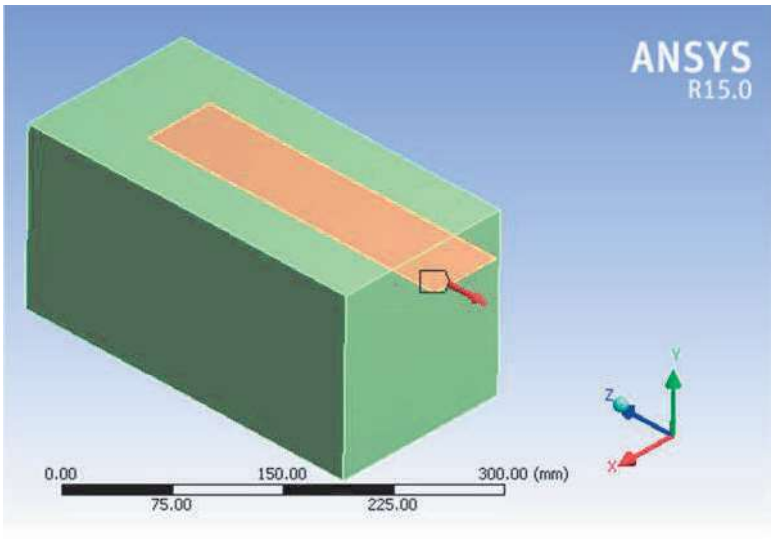

Figure 3.13 Loading Condition of Concrete Specimen with Bonded GFRP (200 mm)

3.2.10 Method Of Analysis

Newton Raphson Method is the most popular technique used in ANSYS for the solution of the Nonlinear equation. In a nonlinear static analysis, the stiffness [K] is reliant on the displacement {x}:

$$[K(x)].\{x\} = \{F\}$$

The subsequent Load/Force vs. Displacement curve may be nonlinear. Therefore, doubling the Load/Force does not necessarily lead to doubling the displacement and stress. A nonlinear

analysis is an iterative approach because it is not recognized beforehand about this connection between load (F) and reaction (x). Therefore, a sequence of linear approximations is conducted with adjustments.

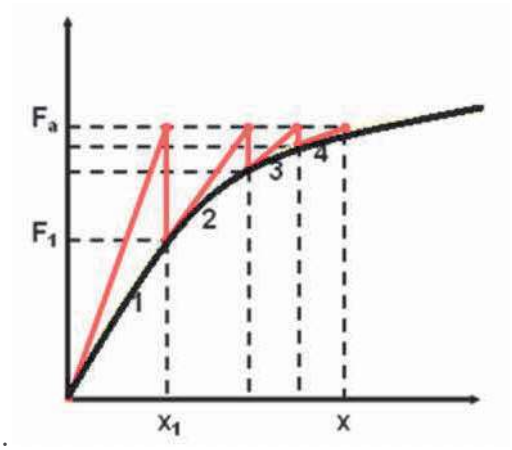

Figure 3.14 Newton Raphson Method

Figure 3.14 explains the Newton Raphson method in a simplified manner (shown as solid red lines)**.** In the Newton Raphson Method, F_a which is the maximum or total load exercised for the first iteration. This result in the corresponding displacement denoted x_1 for the First Iteration. Now from this displacement x_1, the internal force denoted by F_1 can be determined. The system is not in equilibrium $F_a \neq F_1$. Therefore, depending on the present circumstances, a fresh stiffness matrix or slope of the red line is determined. The difference between the forces F_a and F_1 is the out of balance force or the residual forces. For the solution to converge the residual forces must be small enough. This procedure is repeated until the total force F_a becomes equal to the force of the ith Iteration F_i. The system achieves balance for the above example shown in Figure 3.12 after fours iterations and the solution is said to be converged.

CHAPTER 4

RESULTS OF THE FINITE ELEMENT MODELLING

In this chapter, the outcomes from the FEM study are compared with the experimental study which was conducted by Danie Roy et al. (2015). Comparison of Finite element study and experimental study of Load – Slip Behavior of the concrete specimens at various temperatures (Ambient, 200°C, 400°C, 600°C and 800°C), bonded with varying Bond length (100 mm,150 mm and 200 mm) of GFRP is presented below. The outcomes of the Finite Element Study can be seen from the graphs in near agreement with the experimental study. Along with this comparison of effect of bond length on the failure load is also presented in this chapter.

4.1 LOAD – SLIP BEHAVIOR FOR 100 MM BOND LENGTH OF GFRP

Load vs Slip Curve for 100 mm Bond Length of GFRP is presented from Figure 4.1 to Figure 4.5. From all the said Figures it can be noticed that FEM outcomes are close to experimental outcomes initially with a slight deviation as the load progresses. FEM Peak Load is higher than the experimental peak load except for the 800°C case. Also, the curves are becoming flattered with the increase in load.

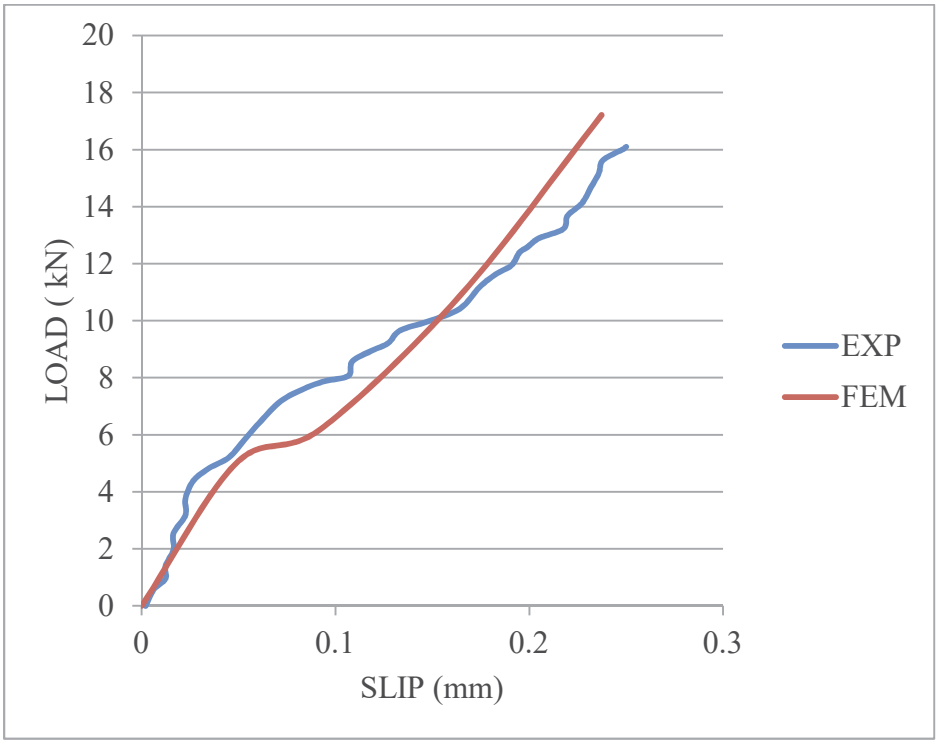

Figure 4.1 Load vs Slip Curve for Bond Length 100 mm, Temperature (Ambient)

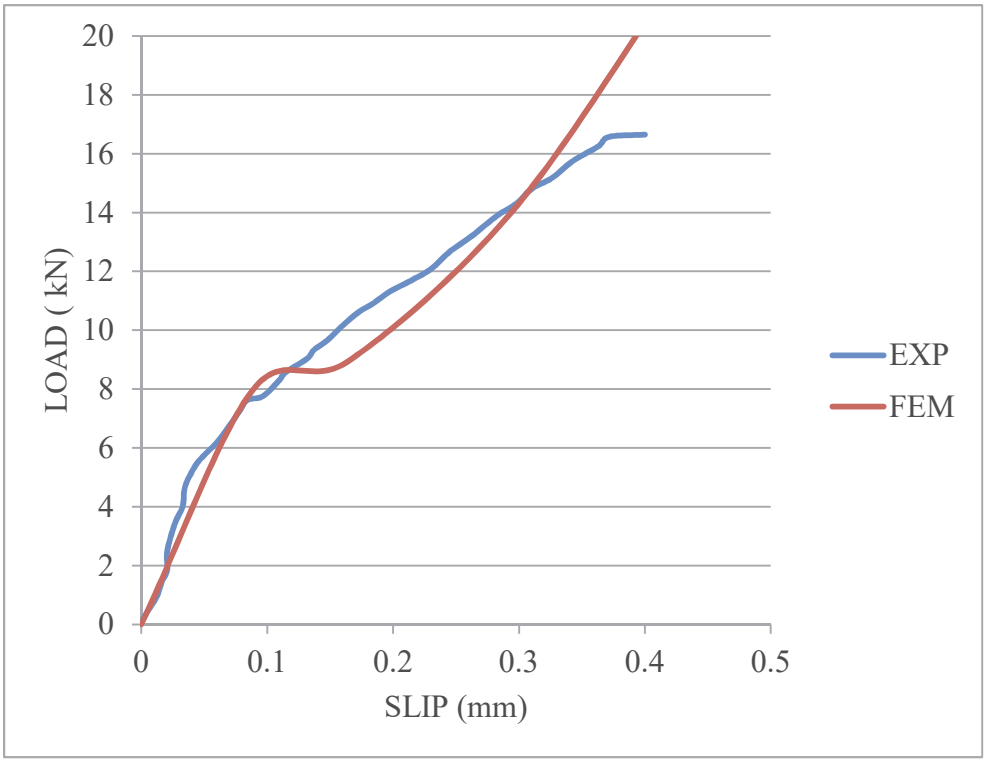

Figure 4.2 Load vs Slip Curve for Bond Length 100 mm, Temperature (200°C)

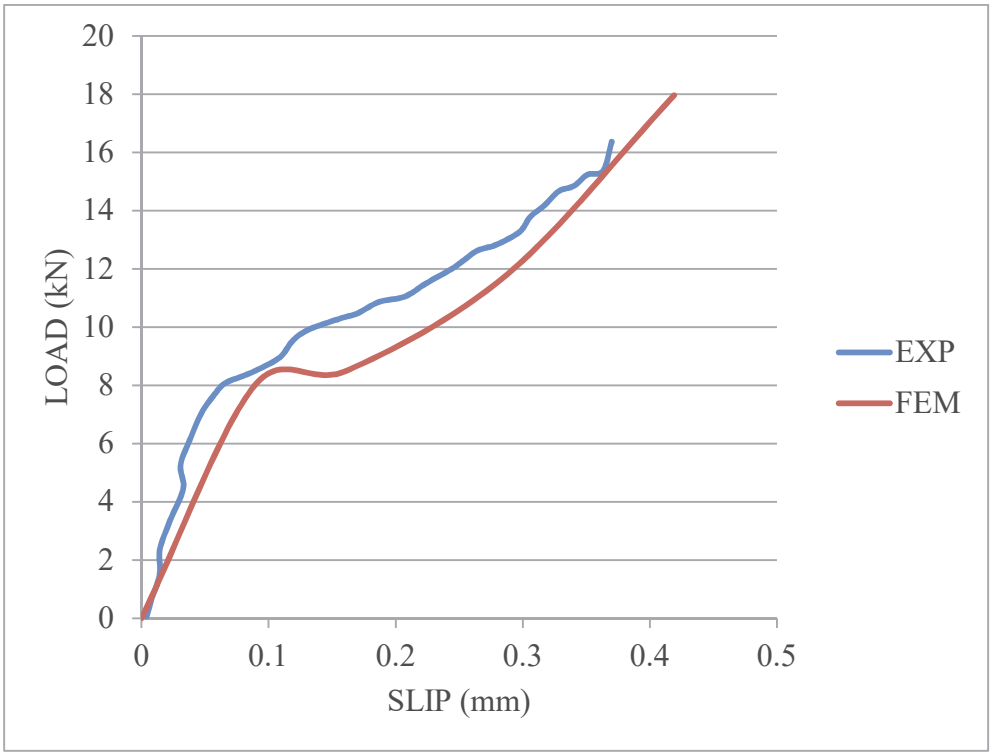

Figure 4.3 Load vs Slip Curve for Bond Length 100 mm, Temperature (400°C)

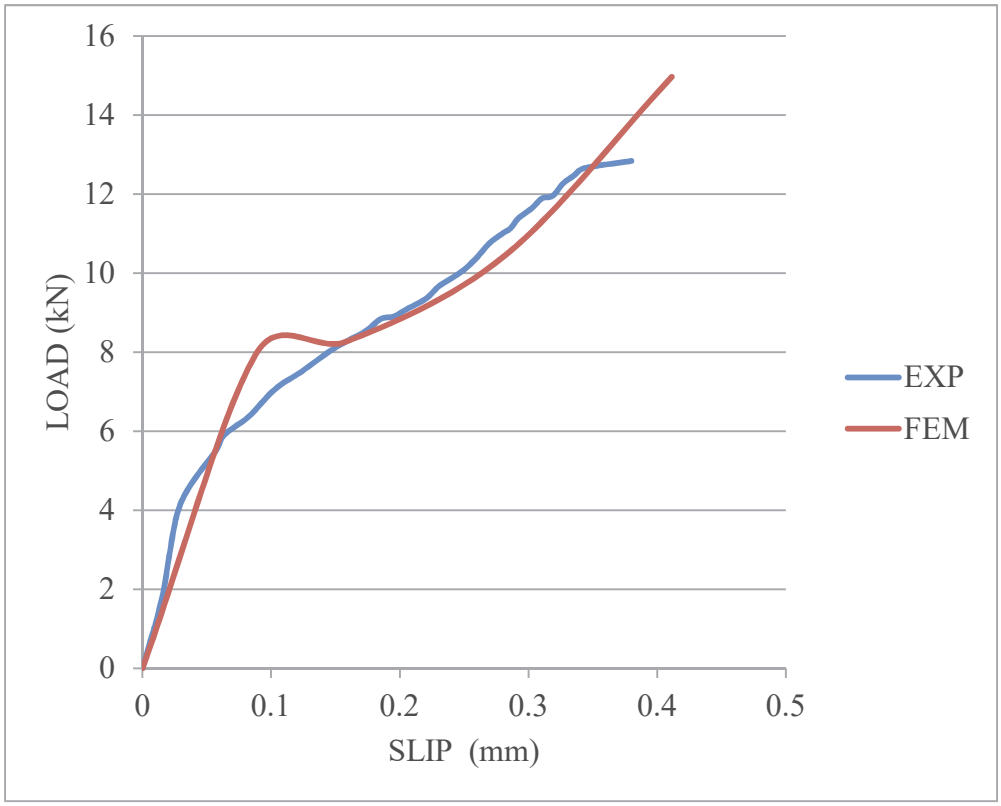

Figure 4.4 Load vs Slip Curve for Bond Length 100 mm, Temperature (600°C)

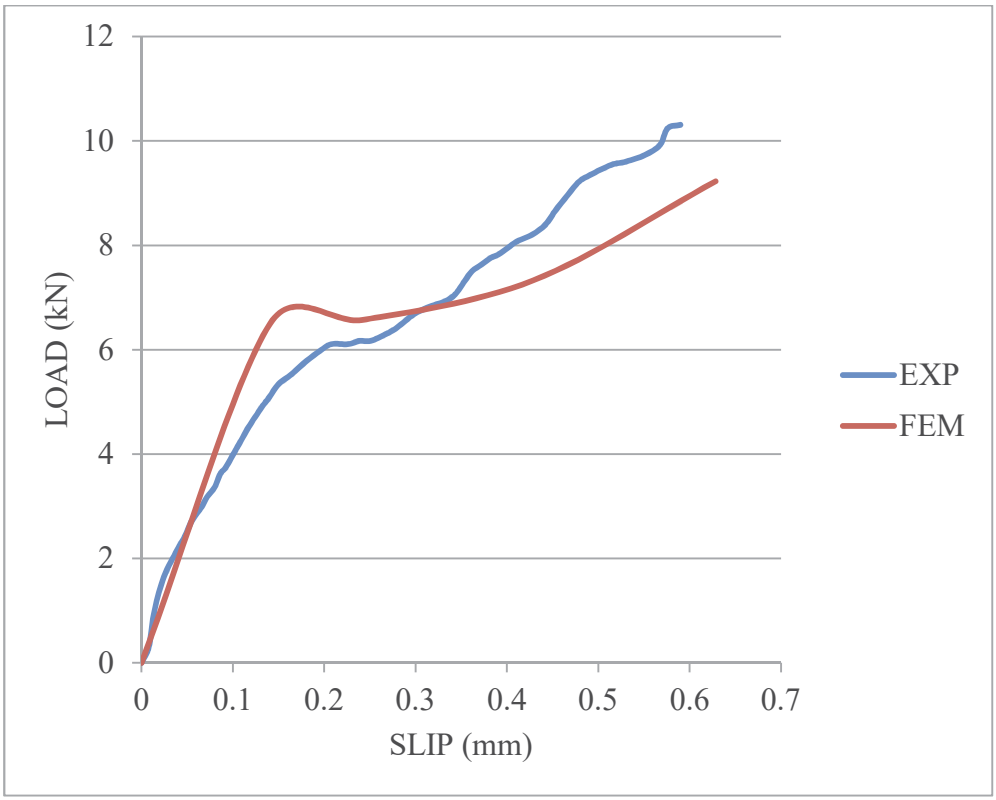

Figure 4.5 Load vs Slip Curve for Bond Length 100 mm, Temperature (800°C)

4.2 LOAD – SLIP BEHAVIOR FOR 150 MM BOND LENGTH OF GFRP

Load – Slip Behavior for 150 mm Bond Length of GFRP is presented from Figure 4.6 to Figure 4.10. From all the said Figures it can be noticed that FEM outcomes are close to experimental outcomes initially with a slight deviation as the load progresses. For the Ambient Temperature case, FEM Load – Slip Behavior is pretty close for the entire region. As noticed for the 100 mm case FEM Peak Load is greater than the experimental peak load except for the 800°C case which is just slightly lower. Flattening of the curves and the decrease in peak load with the rise in temperature is also noticed in this case similar to the 100 mm case.

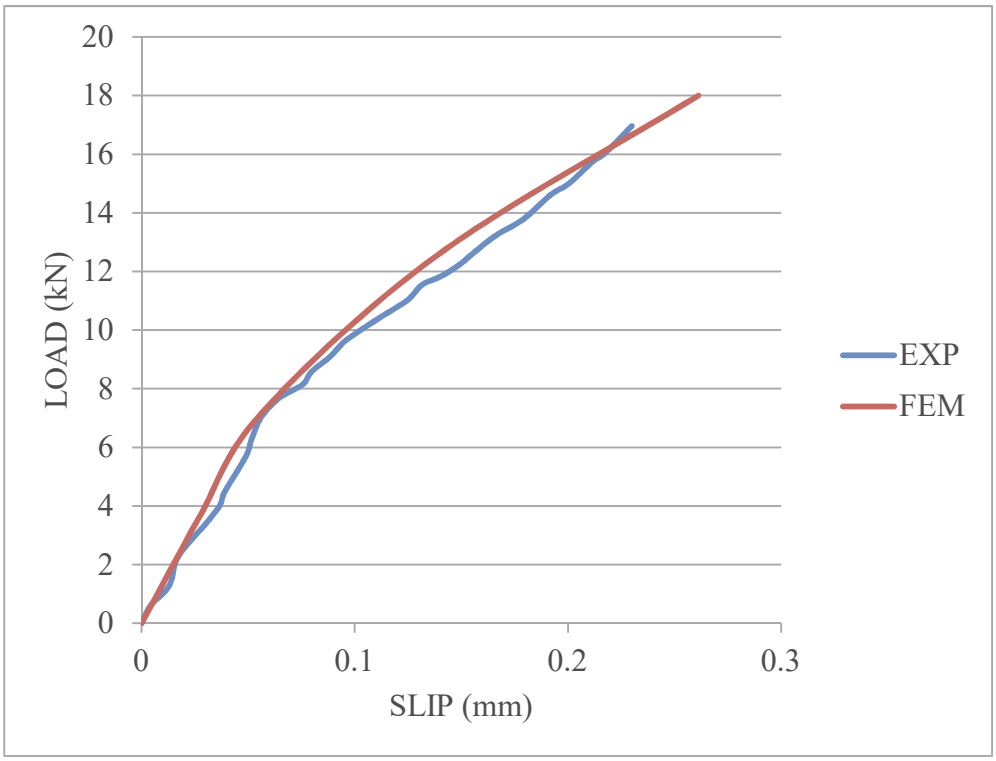

Figure 4.6 Load vs Slip Curve for Bond Length 150 mm, Temperature (Ambient)

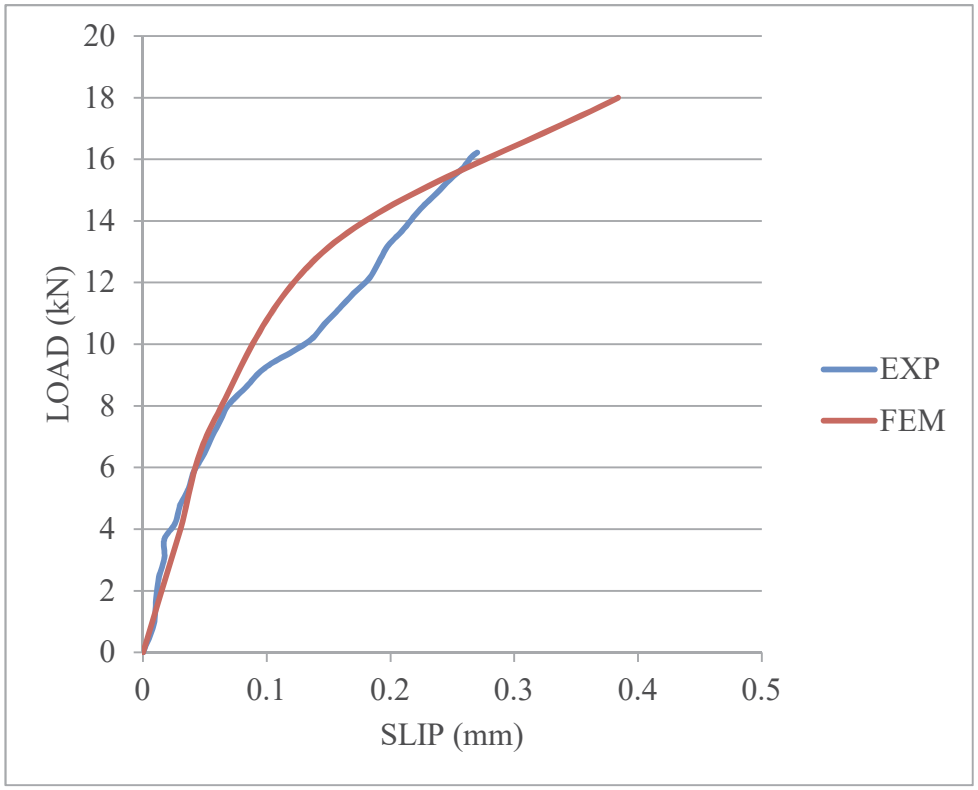

Figure 4.7 Load vs Slip Curve for Bond Length 150 mm, Temperature (200°C)

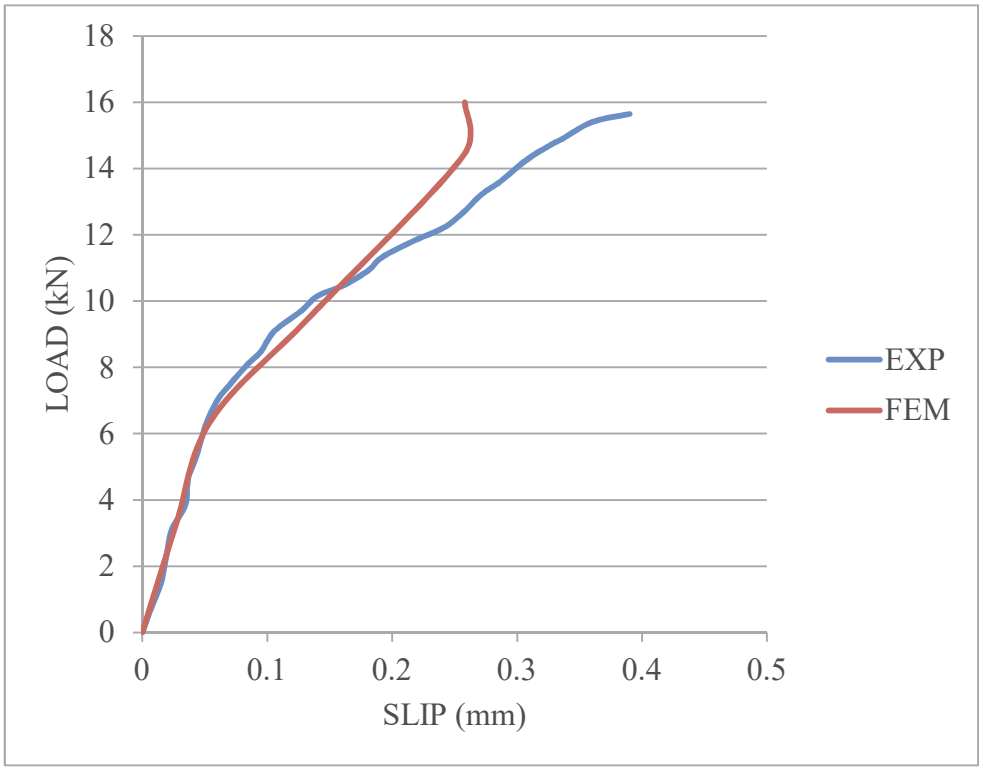

Figure 4.8 Load vs Slip Curve for Bond Length 150 mm, Temperature (400°C)

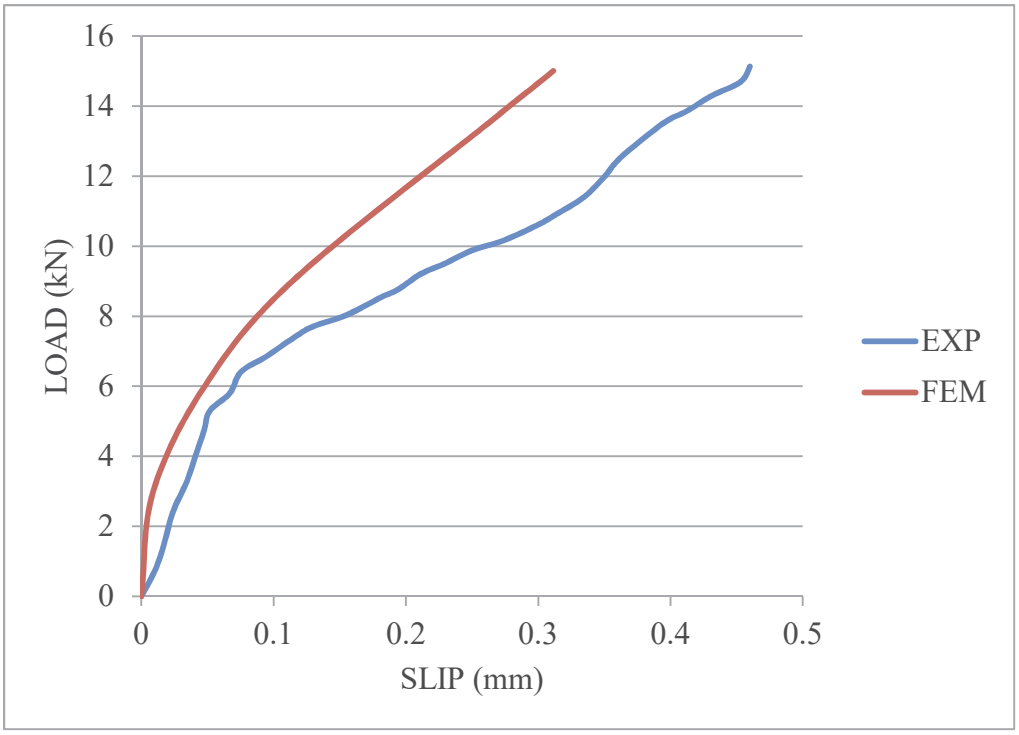

Figure 4.9 Load vs Slip Curve for Bond Length 150 mm, Temperature (600°C)

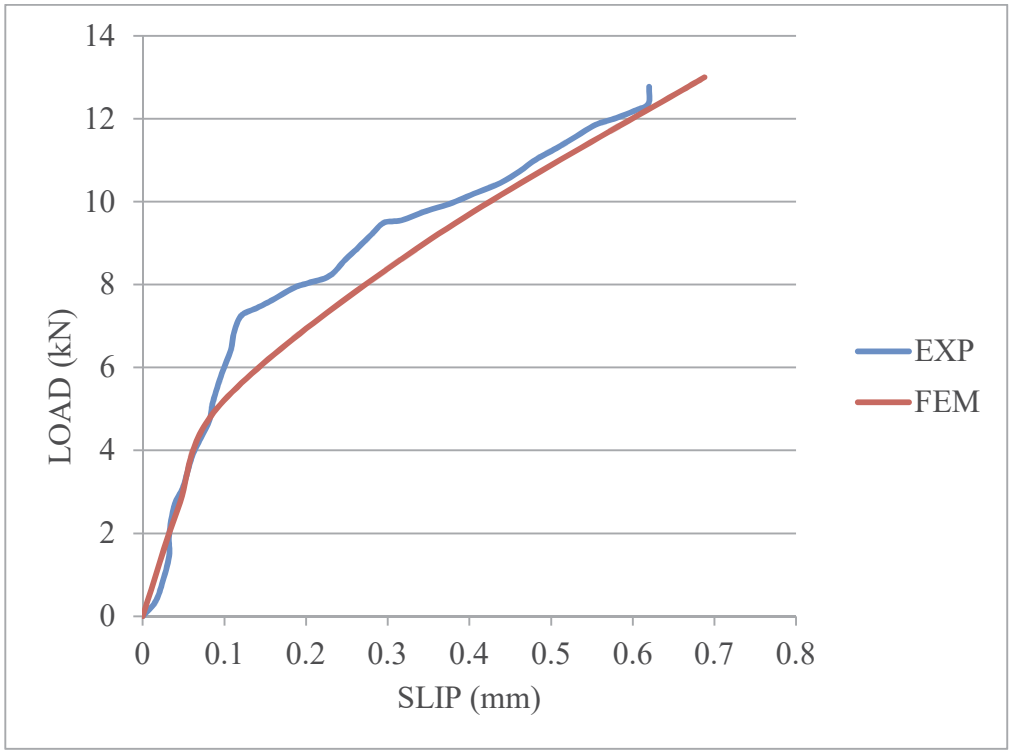

Fig 4.10 Load vs Slip Curve for Bond Length 150 mm, Temperature (800°C)

4.3 LOAD – SLIP BEHAVIOR FOR 200 MM BOND LENGTH OF GFRP

Load – Slip Behavior for 200mm Bond Length of GFRP is presented from Figure 4.11 to Figure 4.15. From all the said Figures it can be noticed that FEM outcomes are close to experimental outcomes initially with the slight deviation as the load progresses except for the ambient temperature case for which there is a slight deviation from the starting. As noticed for the previous cases FEM Peak Load is higher than the experimental peak load with no exceptions. The decrease in peak load with the rise in temperature is noticed but flattening of the curves not that significant as for the experimental case.

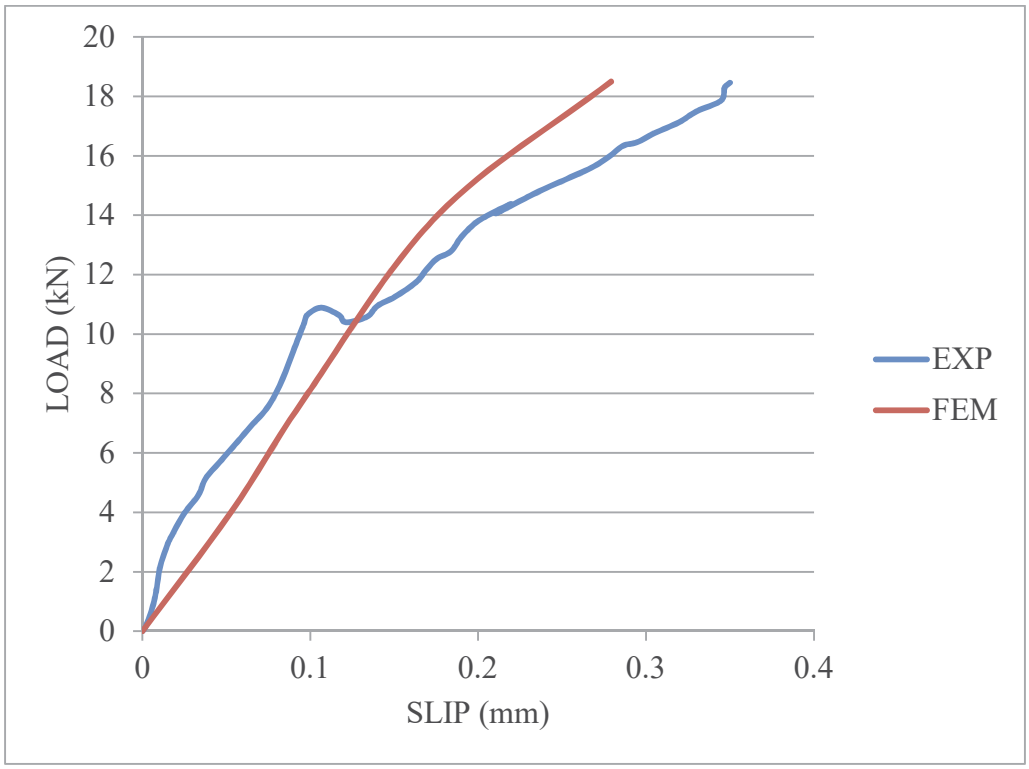

Figure 4.11 Load vs Slip Curve for Bond Length 200 mm, Temperature (Ambient)

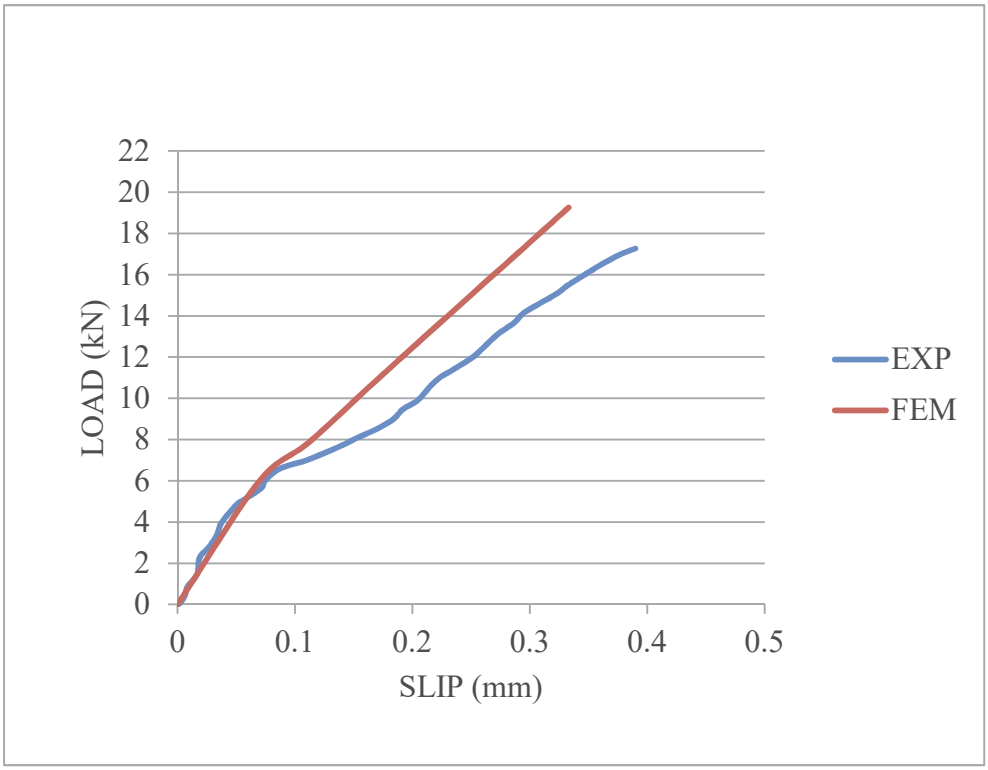

Figure 4.12 Load vs Slip Curve for Bond Length 200 mm, Temperature (200°C)

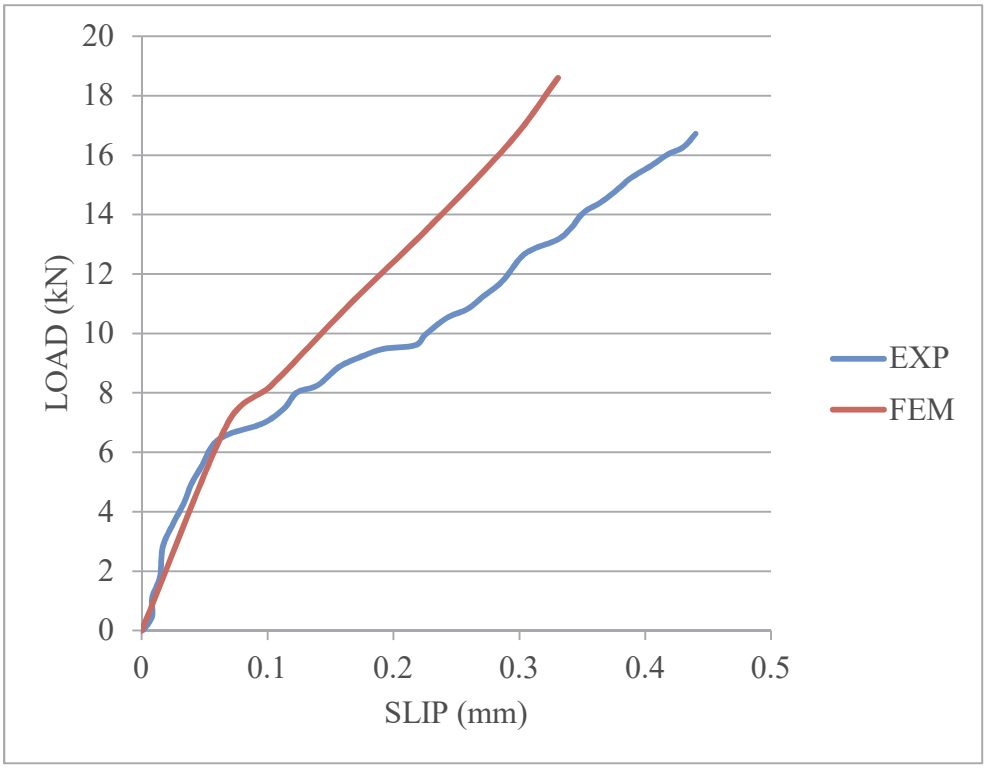

Figure 4.13 Load vs Slip Curve for Bond Length 200 mm, Temperature (400°C)

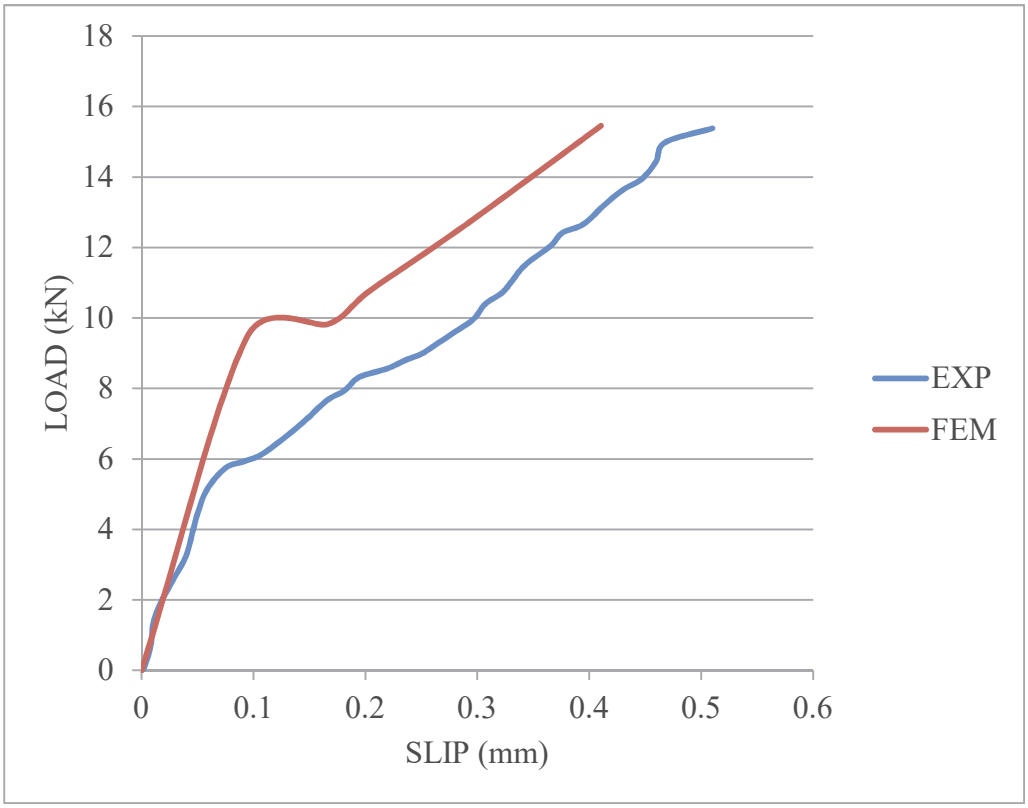

Figure 4.14 Load vs Slip Curve for Bond Length 200 mm, Temperature (600°C)

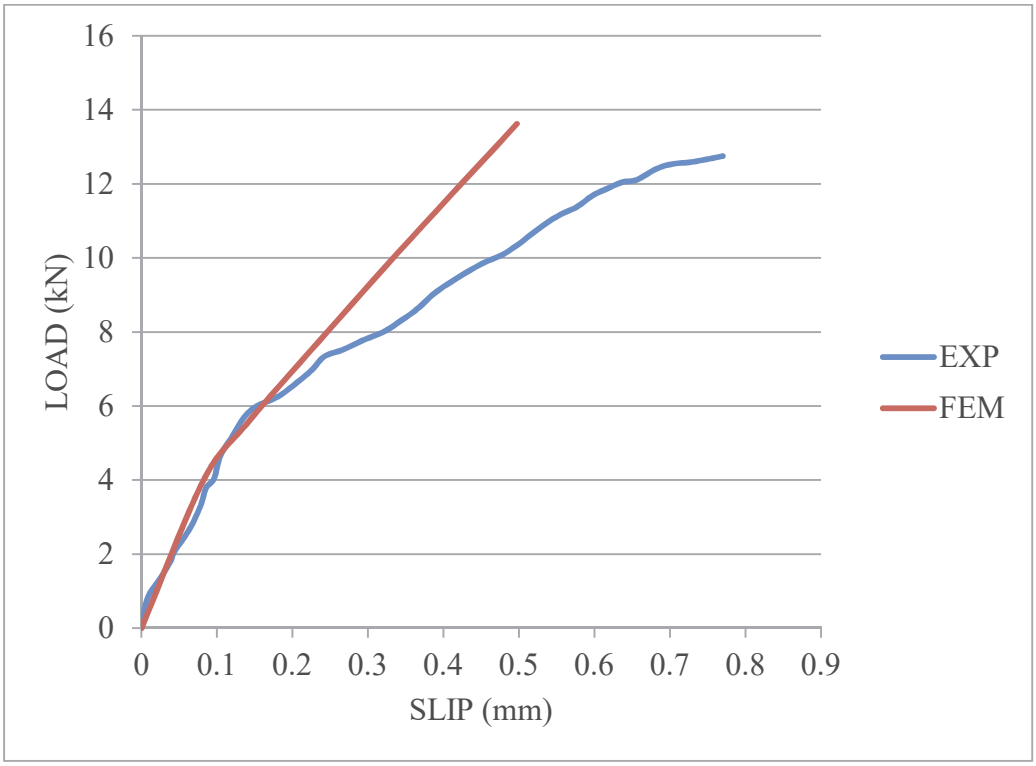

Figure 4.15 Load vs Slip Curve for Bond Length 200 mm, Temperature (800°C)

4.4 COMPARISON OF ULTIMATE BOND STRENGTH AND SLIP OF FEM OUTCOMES WITH EXPERIMENTAL RESULT

Table 4.1 to Table 4.3 shows the Comparison of Ultimate Bond Strength and Slip of FEM Outcomes with Experimental Result for the respective Bond Length of GFRP.

Table 4.1 Comparison Of Ultimate Bond Strength And Slip for 100 mm GFRP Bond Length.

Temperature (°C)	Ultimate Bond Strength, kN EXP	Ultimate Bond Strength, kN FEM	Slip, mm EXP	Slip, mm FEM
Ambient(30)	16.10	17.21	0.25	0.24
200	16.65	22.10	0.40	0.42
400	16.37	17.96	0.37	0.41
600	12.84	14.96	0.38	0.41
800	10.31	9.22	0.59	0.62

Table 4.2 Comparison Of Ultimate Bond Strength And Slip for 150 mm GFRP Bond Length.

Temperature (°C)	Ultimate Bond Strength, kN EXP	Ultimate Bond Strength, kN FEM	Slip, mm EXP	Slip, mm FEM
Ambient(30)	16.96	18.00	0.23	0.26
200	16.22	18.00	0.27	0.38
400	15.65	16.00	0.39	0.25
600	15.13	15.00	0.46	0.31
800	12.77	13.00	0.62	0.68

Table 4.3 Comparison Of Ultimate Bond Strength And Slip for 200 mm GFRP Bond Length.

Temperature (°C)	Ultimate Bond Strength, kN EXP	Ultimate Bond Strength, kN FEM	Slip, mm EXP	Slip, mm FEM
Ambient	18.46	18.50	0.35	0.28
200	17.27	19.26	0.39	0.33
400	16.72	18.60	0.44	0.33
600	15.38	15.45	0.51	0.41
800	12.75	13.62	0.77	0.49

As it can be noticed from the above tables that the Ultimate Bond Strength from the FEM results are comparable to some case while are little high for the other's relative to Ultimate Bond Strength for Experimental Outcomes. The Slip also showed a similar type of behavior owing it to the perfect bond which exists in the Finite element modeling.

Comparing the Ultimate Bond strength for the particular bond length it can be noticed that there is a decrease in it with the increase in temperature. This behavior can be noticed for all the respective bond lengths of the GFRP. This can be credited to the decrease in the tensile strength of the Concrete specimen with the rise in temperature. While comparing the bond strength for different bond length of GFRP for the respective temperatures it can be seen there is an increase in it by increasing the bond length of GFRP. Though the width of GFRP is same but by increasing the length there is an increase in the bond area which leads to the more force transfer from the GFRP laminate to the concrete specimen resulting in higher bond strength.

4.5 COMPARISON OF EFFECT OF BOND LENGTH ON FAILURE LOAD

The comparison of the Effect of Bond Length on Failure Load for the respective Temperature is presented from Figure 4.16 to Figure 4.20. From the Figures it can be noticed that the Failure Load increases with Bond Length for the respective Temperature except for the case of 200°C and 400°C in which failure load declines from 100 mm to 150 mm Bond Length. If the comparison is done Temperature wise there is decrease in Failure Load for the respective Bond Length with the increase in temperature.

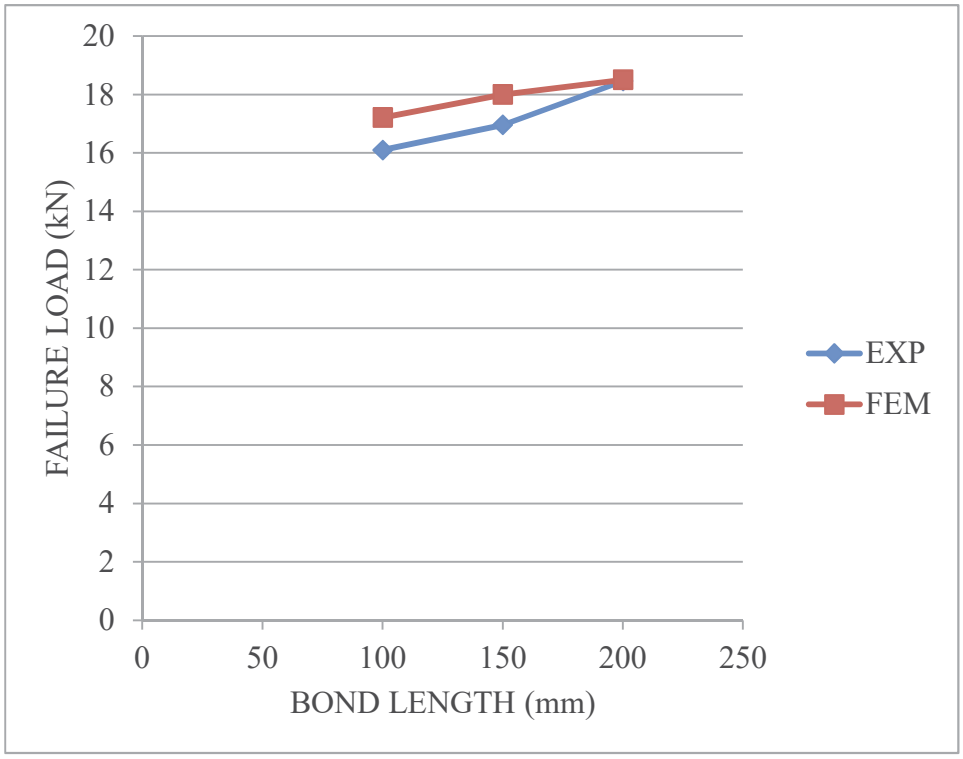

Figure 4.16 Effect of Bond Length on Failure Load, Temperature (Ambient)

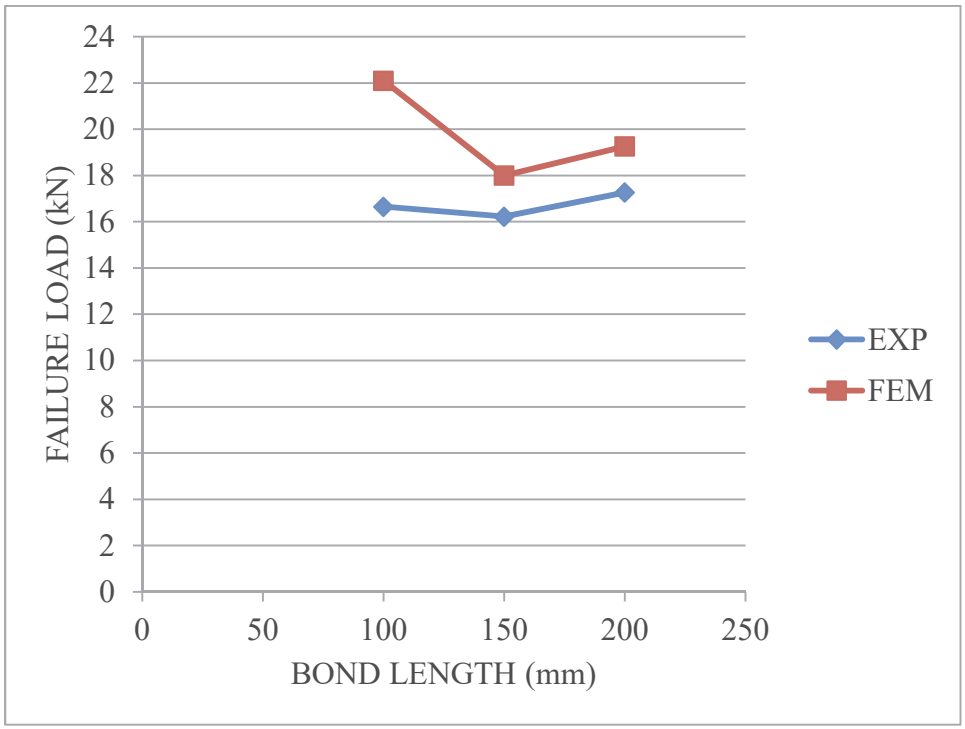

Figure 4.17 Effect of Bond Length on Failure Load, Temperature (200°C)

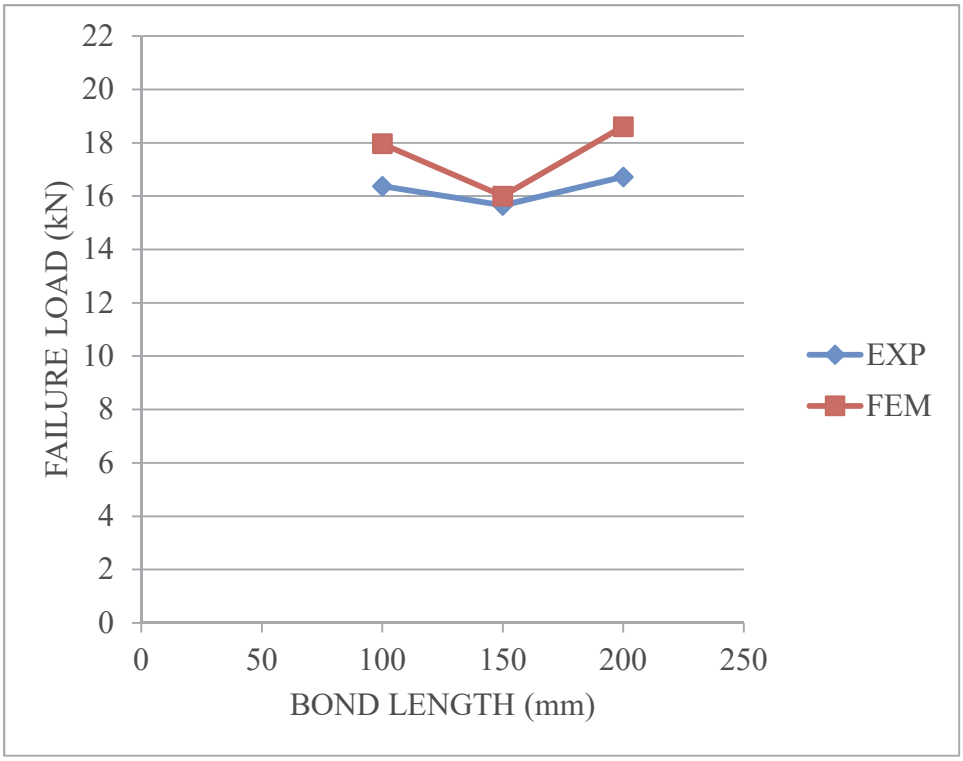

Figure 4.18 Effect of Bond Length on Failure Load, Temperature (400°C)

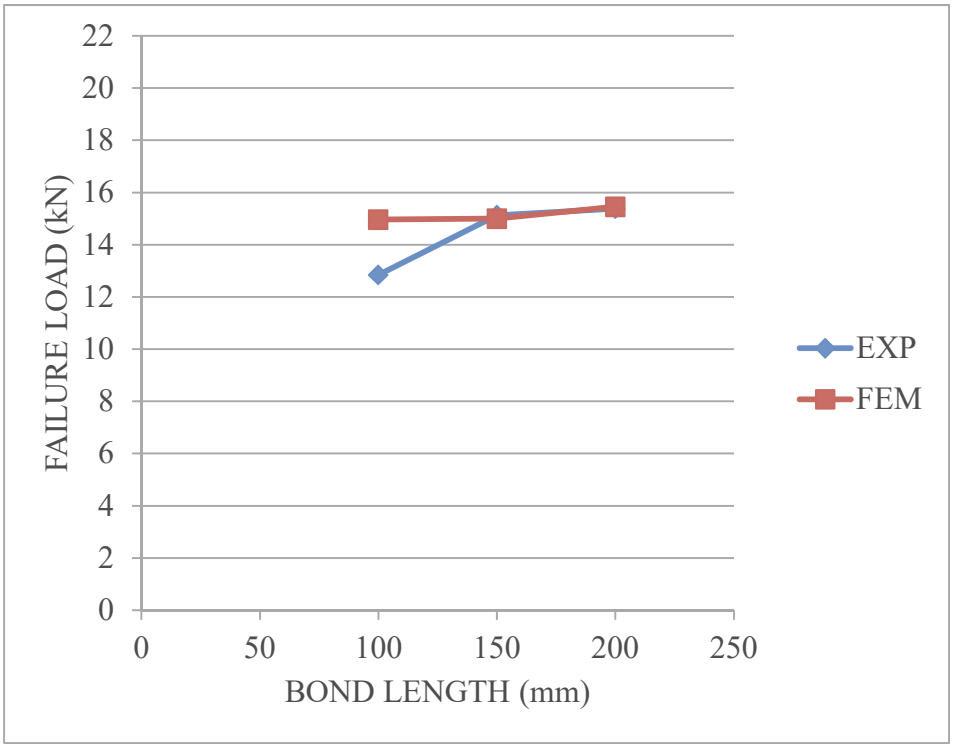

Figure 4.19 Effect of Bond Length on Failure Load, Temperature (600°C)

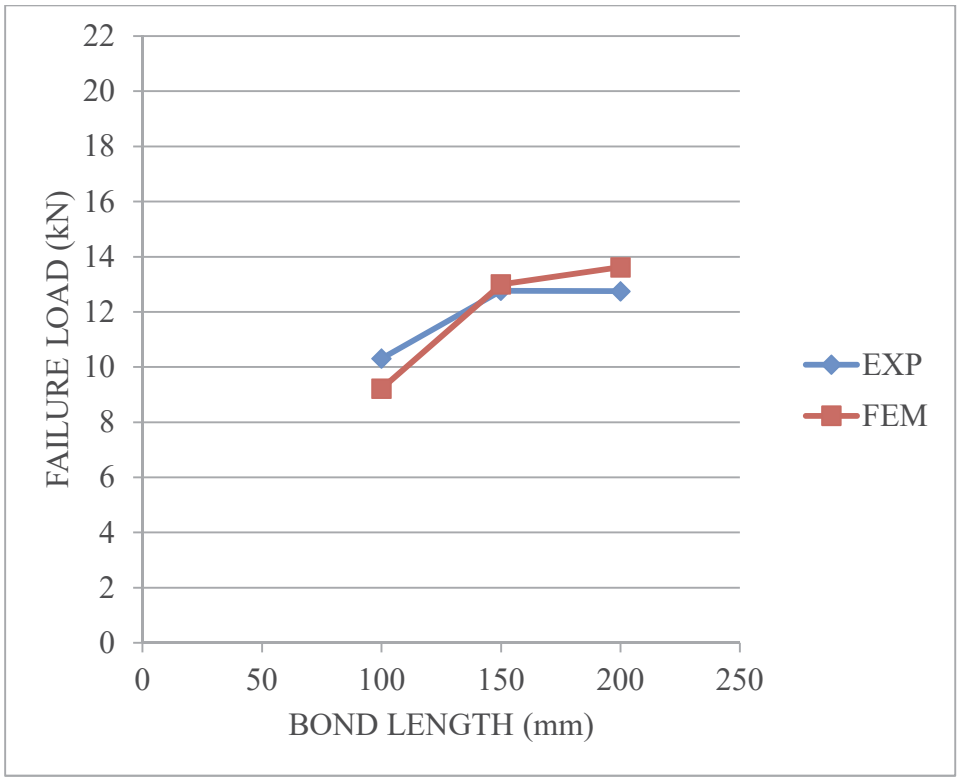

Figure 4.20 Effect of Bond Length on Failure Load, Temperature (800°C)

CHAPTER 5

CONCLUSIONS

Finite element modeling of a heat damaged concrete specimen externally bonded with GFRP was performed in the current research using commercially accessible ANSYS 15.0 software.

5.1 CONCLUSIONS DRAWN FROM THE STUDY

- It is noticed that the FEM analysis is able to predict the Load- slip behavior of heat damaged concrete externally bonded with GFRP.
- As observed from the experimental study Load vs slip behavior was more or less linear up to 400°C, beyond that it showed Non-Linear behavior.
- There was a decrease in Peak Load and increase in Slip with the increasing Temperature owing it to the decrease in Tensile strength of concrete with the rise in temperature.
- With increased bond length regardless of temperature, the ultimate bond strength increases. This can be credited to the increase in the bond area leading to the more load transfer from the GFRP laminate to the concrete specimen.

5.2 FUTURE SCOPE OF THE WORK

For the existent study, FEM is used to simulate the behavior of concrete externally bonded with GFRP. Further studies can be performed on comparative research between distinct FEM software to understand each of the software's accuracies and effectiveness. The use of the different strengthening materials like Carbon fibre reinforced polymer (CFRP), Aramid fibre reinforced polymer (AFRP), etc. can be used and contrasted with the outcomes of the experiment. Other types of test to check the FRP concrete behavior like Double Shear Test, Pull off test, etc. can be used for simulation studies. Near Surface Mounted Retrofit method is also becoming popular these days for strengthening purposes due to its better strength than the externally bonded retrofit method. The same can be used for simulation purposes.

REFERENCES

Abdel Rahman G. Mabrouk and Osman M. Ramadan. "Finite Element Modeling of RC Beams Shear- Strengthened With side bonded CFRP Sheets." APFIS2017 - 6th Asia-Pacific Conference on FRP in Structures. Singapore. 19-21st July (2017).

Agarwal B.D. and Broutman L.J. "Analysis and Performance of Fiber Composites." Published by John Wiley & Sons. Inc. ISBN 0-471-51152-8. (1990): 449.

Arduini, M., & Nanni, A. "Parametric study of beams with externally bonded FRP reinforcement." ACI Structural Journal. 94(5). (1997): 493-501.

Arduini, M., Tommaso, A. D., & Nanni, A. "Brittle failure in FRP plate and sheet bonded beams." ACI Structural Journal. 94(4). (1997): 363-370.

Bizindavyi, L., & Neale, K. W. "Transfer lengths and bond strengths for composites bonded to concrete." ASCE Journal of Composites for Construction. 3(4). (1999): 153-160.

Chajes, M. J., Finch, W. W, Jr, Januszke, T. F., & Thomson, T.A, Jr. "Bond and force transfer of composite material plates bonded to concrete." ACI Structural Journal. 93(2). (1996): 208-217.

Chen, J. F., and Y. Tao. "Finite element modelling of FRP-to-concrete bond behaviour using the concrete damage plasticity theory combined with a plastic degradation model." In Advances in FRP Composites in Civil Engineering. Springer. Berlin. Heidelberg. (2011): 45-50.

Chowdhury , Fazlul Habib and Islam , G M Sadiqul. "Application of FRP Materials for Strengthening of RC Structural Members." 2nd International Conference on Advances in Civil Engineering. (ICACE-2014). Chittagong. Bangladesh. (2014).

Danie Roy, A. B., Sharma, U. K., and Bhargava, P. " Strengthening of heat damaged reinforced concrete short columns." J. Struct. Fire Eng. 5(4). (2014): 381-398.

Danie Roy, A. B., U. K. Sharma, and P. Bhargava. "Bond Properties of GFRP Laminate with Heat-Damaged Concrete." Journal of Composites for Construction. 20(2). (2015): 04015053.

FIB. "Externally bonded FRP reinforcement for RC structures Technical Report." Task Group 9.3 FRP (Fibre Reinforced Polymer) reinforcement for concrete structures. Bulletin 14. ISBN 2-+88394-054-1. July (2001): 130.

Haddad, R. H., Al-Rousan, R., and Almasry, A. "Bond-slip behavior between carbon fiber reinforced polymer sheets and heat-damaged concrete." Composites Part B. 45(1). (2013): 1049-1060.

Harmon, T. G., Kim, Y. J., Kardos, J., Johnson, T., & Stark, A. “Bond of surface mounted fiber-reinforced polymer reinforcement for concrete structures.” ACI Structural Journal. 100(5). (2003): 557-564.

Hind, M. Kh, M. Özakçab, and T. Ekmekyaparc. “A Review on Nonlinear Finite Element Analysis of Reinforced Concrete Beams Retrofitted with Fiber Reinforced Polymers.” J. Adv. Res. Appl. Mech 22 (2016): 13-48.

Ibrahim, A.M., and Mahmood, M.S. “Finite Element Modeling of Reinforced Concrete Beams Strengthened with FRP Laminates.” European Journal of Scientific Research. 30(4). (2009): 526-541.

IS 456: 2000 (Fourth Revision), “Indian Standard: Plain and Reinforced Concrete – Code of Practice”, Bureau of Indian Standards, New Delhi, 2005.

Kang, Thomas H-K., Joe Howell, Sanghee Kim, and Dong Joo Lee. “A state-of-the-art review on debonding failures of FRP laminates externally adhered to concrete.” International Journal of Concrete Structures and Materials 6(2). (2012): 123-134.

Klamer, E. “The influence of temperature on concrete structures strengthened with externally bonded CFRP.”Research Rep., Eindhoven Univ. of Technology, Eindhoven, Netherlands. (2006).

Leone, M., Matthys, S., and Aiello, M. A. “Effect of elevated service temperature on bond between FRP EBR systems and concrete.” Composites Part B. 40(1). (2009): 85-93.

López-González, Julio C., Jaime Fernández-Gómez, and Enrique González-Valle. “Effect of adhesive thickness and concrete strength on FRP-concrete bonds.” Journal of Composites for Construction 16(6). (2012): 705-711.

Madenci, Erdogan, and Ibrahim Guven. The Finite Element Method and Applications in Engineering Using ANSYS®. Springer, (2015).

Ma Q, Guo R, Zhao Z, Lin Z, He K. “Mechanical properties of concrete at high temperature A review.” Construction and Building Materials. (2015) Sep 15;93: 371-83.

Mazzotti. C, Savoia. M, and Ferracuti B. “An experimental study on delamination of FRP plates bonded to concrete.” Construction and Building Materials 22 (2008): 1409-1421

Miller, Brian, and Antonio Nanni. “Bond between CFRP sheets and concrete.” Proceedings ASCE 5th Materials Congress. (1999).

Mohamed, Osama Ahmed, and Rania Khattab. “Bond-slip Modelling of FRP Sheets Externally Bonded to Concrete Beam.” Procedia engineering 161 (2016): 833-838.

Mukhtar, Faisal M., and Rayhan M. Faysal. “A review of test methods for studying the FRP concrete interfacial bond behavior.” Construction and Building Materials 169 (2018): 877-887.

Nakaba, K., Kanakubo, T., Furuta, T., and Yoshizawa, H. “Bond behavior between fiber-reinforced polymer laminates and concrete.” ACI Struct. J. 98(3). (2001). 359-367.

Ouezdou, Mongi Ben, Abdeldjelil Belarbi, and Sang-Wook Bae. “Effective bond length of FRP sheets externally bonded to concrete.” International Journal of Concrete Structures and Materials 3(2). (2009): 127-131.

Pellegrino C. and Modena C. “Bond-Slip Relationship between FRP Sheets and Concrete.” Fourth International Conference on FRP Composites in Civil Engineering (CICE2008). Zurich. Switzerland. July (2008): 22-24.

Pham B. H. and Al-Mahaidi R. “Modelling of CFRP-Concrete Shear-Lap Tests.” Construction and Building Materials 21 (2007): 727-735.

Saito M. and Kobayashi A. “Development and Application of Continuous Fiber Reinforced Materials for Concrete Structures.” Nippon Steel Composite Co. Ltd. (Personal correspondence). (2000).

Sayed-Ahmed, E. Y., R. Bakay, and N. G. Shrive. “Bond strength of FRP laminates to concrete: state-of-the-art review.” Electronic Journal of structural engineering 9(1). (2009): 45-61.

Seo, Soo-Yeon, Luciano Feo, and David Hui. “Bond strength of near surface-mounted FRP plate for retrofit of concrete structures.” Composite Structures 95 (2013): 719-727.

Swamy R.N. and Mukhopadhyaya P. (1999). “Debonding of Carbon-Fiber- Reinforced Polymer Plate from Concrete Beams.” Proc. Instn Civ. Engrs Structs & Bldgs. 134 Nov. (1999): 301-317. Paper 11961.

Tarek Alkhrdaji, P.(2019). STRUCTURE magazine. Strengthening of Concrete Structures Using FRP Composites. Available at: https://www.structuremag.org/?p=8643 (Accessed 14 Jul. 2019).

Täljsten B. “Plate Bonding, Strengthening of Existing Concrete Structures with Epoxy Bonded Plates of Steel or Fibre Reinforced Plastics.” Doctoral Thesis. 152D, ISSN 0348-8373. Luleå University of Technology. (1994): 308.

Teng J. G., Chen J. F., Smith S. T., & Lam L. “Behaviour and strength of FRP strengthened RC structures: a state-of-the-art review.” Proceedings of the ICE-Structures and Buildings. 156(1). (2003): 51-62.

Teng J.G. and Chen J.F. (2007). “Debonding Failures of RC Beams Strengthened with Externally Bonded Reinforcement: Behavior and Modelling.” Asia-Pacific Conference on FRP

in Structures (APFIS 2007). S.T. Smith (ed). International Institute for FRP in Construction. (2007).

Turner, M. J.,Clough, R. W., Martin, H. C, and Topp, L. J. “Stiffness and Deflection Analysis of Complex Structures.” Journal of the Aeronautical Sciences. 23. (1956): 805-823.

Xiao, J., Li, J., and Zha, Q. “Experimental study on bond behaviour between FRP and concrete.” Constr. Build. Mater. 18(10). (2004): 745-752.

Yao, J., Ting, J. G., and Chen, J. F. “Experimental study on FRP-to- concrete bonded joints.” Composites Part B. 36(2). (2005): 99-113.

bond behaviour and fem analysis ANSHUL SANDHU(801724005)

ORIGINALITY REPORT

11%	4%	6%	9%
SIMILARITY INDEX	INTERNET SOURCES	PUBLICATIONS	STUDENT PAPERS

PRIMARY SOURCES

1	Submitted to Higher Education Commission Pakistan Student Paper	1%
2	"Advances in FRP Composites in Civil Engineering", Springer Nature, 2011 Publication	1%
3	Kang, Thomas H.-K., Joe Howell, Sanghee Kim, and Dong Joo Lee. "A State-of-the-Art Review on Debonding Failures of FRP Laminates Externally Adhered to Concrete", International Journal of Concrete Structures and Materials, 2012. Publication	1%
4	Submitted to Universiti Tenaga Nasional Student Paper	1%
5	Submitted to National Institute of Technology, Rourkela Student Paper	1%
6	Submitted to University of Pretoria Student Paper	1%